

MARS CLIMATE DATABASE v5.3 DETAILED DESIGN DOCUMENT

(ESA Contract No. 4000117944/16/NL/LF/as)

CNES Contract "Base de données climatique martienne"

F. Forget, E. Millour, M. Vals, V. Zakharov (LMD) and S.R. Lewis (OU)

July 2017

Abstract

This is the Detailed Design Document for version 5.3 of the Mars Climate Database (MCD). It contains a detailed description of the database and addresses technical aspects of how the data is represented, manipulated and post-processed by the MCD access software. Instructions on how to install the MCD and use the provided access software and post-processing tools are given in the MCD v5.3 **User Manual**.

Contents

1	Introduction	3
2	General Description of Database Contents	4
2.1	MCD Files	4
2.2	MCD Software	4
2.3	MCD Datasets and Datafiles	4
2.4	Database Grid Structure	7
2.4.1	Horizontal Structure	7
2.4.2	Vertical Structure	8
2.4.3	Temporal Structure	9
3	Dust Distribution and EUV Scenarios in the MCD	10
3.1	The EUV Scenarios	11
3.2	The Dust Scenarios	12
3.2.1	Parametrization of dust vertical distribution and particle size variations	12
3.2.2	Prescribed dust column optical depth variations	12
4	Technical description of Methods Used to Retrieve Data from the MCD	16
4.1	Temporal Interpolations	16
4.2	Spatial Interpolations	16
4.2.1	Horizontal Interpolation	16
4.2.2	Vertical Interpolation	16
4.2.3	Specific Treatments of Vertical Interpolation	17
5	Variability Models in the MCD	18
5.1	Day-to-Day RMS of Variables	18
5.2	The Large-Scale Variability Model	18
5.2.1	Calculation of EOFs and PCs	19
5.2.2	Storage of variability with EOFs	20
5.2.3	Reconstructing a realistic variability	20
5.2.4	Reconstructing the inter-annual variability of the Martian atmosphere	21
5.3	The Small-Scale Variability Model	23
6	High Resolution Outputs	25
6.1	High Resolution Topography and Areoid	25
6.1.1	Mars Gravity Model	25
6.1.2	MOLA Topography	25
6.2	Deriving High Resolution Surface Pressure	26
6.2.1	Deriving high resolution pressure for the dust storm cases	26
6.3	Computing High Resolution Values of Atmospheric Variables	27
6.3.1	Interpolation of Atmospheric Temperature	27
6.3.2	Interpolation of Density	29
6.3.3	Modification of Other Variables	29
A	Computing Martian Dates and Local Time	32
A.1	Some constants	32
A.2	Computing martian dates and aerocentric solar longitude	32
A.2.1	The three anomalies	32
A.2.2	Aerocentric solar longitude L_s	32
A.2.3	Converting Julian date JD to Martian sol number D_s	33
A.2.4	Converting sol number D_s date to L_s	33
A.3	Computing Local True Solar Time	33
B	Differences Between Version 5.3 and Previous Versions of the MCD	35

1 Introduction

The Mars Climate Database (MCD) is a database of atmospheric statistics compiled from state-of-the-art Global Climate Model (GCM) simulations of the Martian atmosphere.

The GCM computes in 3D the atmospheric circulation taking into account radiative transfer through the gaseous atmospheres as well as through dust and ice aerosols, includes a representation of the CO₂ ice condensation and sublimation on the ground and in the atmosphere, simulates the water cycle (with modelling of cloud microphysics), the dust multisize particle transport, the atmospheric composition controlled by the photochemistry and the local non-condensable gas enrichment and depletion induced by CO₂ condensation and sublimation. It has been extended into the thermosphere and model the ionospheric processes¹.

The model used to compile the statistics has been extensively validated using available observational data and aims at representing the current best knowledge of the state of the Martian atmosphere given the observations and the physical laws which govern the atmospheric circulation and surface conditions on the planet.

The Mars Climate Database access software adds several capabilities to better represent the Martian environment variability and accurately compute the surface pressure at high spatial resolution.

This document provides the user of the MCD with a detailed description of the database structure and of technical aspects of the access software.

The MCD is freely available online at request. Its content may also be accessed to make plots and figures using the interactive server on our WWW site at:

¹. A detailed description of the LMD Global Climate Model is out of the scope of the present document. Nevertheless, details can be found in the scientific papers provided with the database in the `docs/articles` directory:

- `model_jgr99.pdf` : Reference description of the General Circulation Model used to make the Mars Climate Database (MCD) v1 (somewhat obsolete, but useful)
- `mcd.v1.0-jgr99.pdf` : Description of the MCDv 1.0 (somewhat obsolete, but useful).
- `dust_distribution_jgr2011.pdf` : Description of how the dust distribution is prescribed in the MCD v5 and validation with MGS TES observations.
- `dust_climatology_icarus2015.pdf` : How the available dust opacity observations have been compiled to create the dust scenarios used to simulate Martian Years 24 to 31 in MCD v5.
- `water_clouds_jgr2004.pdf` : Includes a description of the water vapor, water cloud model used for MCD v4. (somewhat obsolete, but useful)
- `water_clouds_gr12013.pdf` : Describes the modeling of the radiatively active clouds (as done in MCD v5) and analyses their influence.
- `water_clouds_jgr2014.pdf` : Further description and details on the modeling of the water cycle with radiatively active clouds and an improved cloud microphysical model.
- `convection_pbl_jgr2013.pdf` : Describes the improved parametrisation of the turbulent/convection dynamics used for MCD v5.
- `ozone_jgr2004.pdf` : The chemistry-transport model used to predict ozone (MCD v4)
- `ozone_nature2008.pdf` : More recent results from the chemistry-transport model used to predict ozone (MCD v5)
- `non_condensable_gas_2008.pdf` : An extended abstract describing the modeling of the non-condensable gas enrichment and depletion induced by the condensation and sublimation of CO₂ in MCD v5.
- `thermosphere_gr105.pdf` : Extension of the GCM to the thermosphere as done in MCD v4.
- `thermosphere_jgr2009.pdf` : A more detailed description of the extension of the GCM in the thermosphere as done in MCD v4.
- `thermosphere_variability_jgr2015.pdf` : Analysis and validation of the thermosphere variability simulated by the GCM from MY24 to MY31.
- `ionosphere_jgr2013.pdf` : A description of the photochemical ionosphere (from surface up to ~180km) in the model.

<http://www-mars.lmd.jussieu.fr>

2 General Description of Database Contents

2.1 MCD Files

The MCD main directory contains three folders: `docs` which contains documentation, `data` which contains the datafiles and `mcd` which contains the access software (see the User Manual).

2.2 MCD Software

Subdirectory `mcd` contains the following Fortran programs:

- `call_mcd.F`: This is the main subroutine which should be used to retrieve data from the database. The file also contains a collection of subsidiary routines. It requires the include file `constants_mcd.inc` to run and also uses subroutine `heights.F`. Input and output arguments of `call_mcd` are documented in the MCD User Guide.
- `heights.F`: This subroutine performs conversions between different height coordinates (namely altitude above local surface, above areoid or distance to the center of planet). It is used by `call_mcd.F` and has only been kept separate from the rest of the subroutines as a facility for some users.
- `julian.F`: A subroutine which converts Earth date into the corresponding Julian date (one of the forms of date input used by `call_mcd`).
- `test_mcd.F`: A sample program provided to display (and test) the way to call subroutine `call_mcd` and to retrieve data from the MCD.

The `pres0` subdirectory also contains a post-processing subroutine, `pres0.F`, which can be used to retrieve high resolution surface pressure. This feature is also implemented in `call_mcd`, which makes this utility redundant. It has however been retained in the MCD distribution for users who are only interested in retrieving high resolution surface pressure and require a minimal and light tool to do so.

Apart from these Fortran programs, the `mcd` directory also contains subdirectories which examples of interfaces for other languages: `idl`, `matlab`, `scilab`, `python` and `c_interfaces` (which contains both C and C++ interface examples). See the accompanying README files and the MCD User Manual for details.

2.3 MCD Datasets and Datafiles

MCD data is stored in various folders and files in directory `data` using the Network Common Data Form (NetCDF) developed and distributed by Unidata. The NetCDF libraries are freely available for numerous platforms from the Unidata web site:

<http://www.unidata.ucar.edu/software/netcdf>

- Essential and common datafiles
 - File `mountain.nc` which contains maps (at model resolution, i.e. a 64x49 longitude-latitude grid) of topography, areoid and sub-gridscale standard deviation of topography (useful for computing gravity wave perturbations).
 - File `mola32.nc` which contains a high resolution (32 pixels per degree) map of Martian topography.

- File `mgm1025` contains the spherical harmonic expansion coefficients necessary to compute the Martian areoid with high accuracy.
 - File `VL1.ls` contains a diurnally averaged and smoothed record of surface pressure at Viking Lander 1 site.
 - File `VL3.ls` contains a diurnally averaged and smoothed record of surface pressure at (a fictitious) Viking Lander 3 site. This data is specifically used for pressure corrections in high resolution mode with the dust storm scenarios (see section 6.2).
 - File `ps_clim.nc` contains a minimal subset of MCD data which is used by the standalone 'pres0' tool.
- Individual dust scenarios (see section 3 for a detailed description) datafiles are in corresponding subdirectories:
 - `clim_aveEUV`, `clim_minEUV` and `clim_maxEUV` for the baseline climatology² dust scenarios,
 - `cold` for the cold scenario
 - `warm` for the warm scenario
 - `strm` for the dust storm scenario
 - `MY24`, `MY25`, `MY26`, `MY27`, `MY28`, `MY29`, `MY30`, `MY31` and `MY32` for the Martian Year scenarios.

The file naming convention for each file is as follows :

Data Filename = 'scen'_'mon'_'type'.nc for low atmospheric files (up to around 130km – 30 levels)
 Data Filename = 'scen'_'mon'_'thermo_'solar'_'type'.nc for thermospheric files (from around 130km up to around 300km – 19 levels).

'scen' denotes the dust scenario type (`clim`, `cold`, `warm`, `strm`, `MY24`, `MY25`, etc.), where 'mon' denotes the month number:

- 'mon' = '01' is month 1, $L_s = 0^\circ - 30^\circ$,
- 'mon' = '02' is month 2, $L_s = 30^\circ - 60^\circ$,
- 'mon' = '03' is month 3, $L_s = 60^\circ - 90^\circ$,
- 'mon' = '04' is month 4, $L_s = 90^\circ - 120^\circ$,
- 'mon' = '05' is month 5, $L_s = 120^\circ - 150^\circ$,
- 'mon' = '06' is month 6, $L_s = 150^\circ - 180^\circ$,
- 'mon' = '07' is month 7, $L_s = 180^\circ - 210^\circ$,
- 'mon' = '08' is month 8, $L_s = 210^\circ - 240^\circ$,
- 'mon' = '09' is month 9, $L_s = 240^\circ - 270^\circ$,
- 'mon' = '10' is month 10, $L_s = 270^\circ - 300^\circ$,
- 'mon' = '11' is month 11, $L_s = 300^\circ - 330^\circ$,
- 'mon' = '12' is month 12, $L_s = 330^\circ - 360^\circ$,

'mon' = 'all' is the whole year for the Empirical Orthogonal Functions (EOF) data for the large-scale variability model.

'type' indicates the type of data in the file :

- 'type' = 'me' means "mean data",
- 'type' = 'sd' means "standard deviation data" and "rms data",
- 'type' = 'eo' means EOF data for large scale perturbations.

'solar' indicates the type of solar scenario for thermosphere files:

- 'solar' = 'min' for fixed minimum EUV,
- 'solar' = 'ave' for fixed average EUV,

²Note that only the `clim_aveEUV` directory is required; all others are optional, in the sense that they are only required when data for these specific scenarios is sought.

‘solar’ = ‘max’ for fixed maximum EUV,
‘solar’ = ‘var’ for varying (ie. daily evolving) EUV.

Each of the m_e mean data files contain 12 mean values (for the given month) corresponding to 12 solar times of day (i.e. every 2 hours) for the variables shown in Table 1. The sd data files contain day-to-day RMS values of variables (see Table 2 for details).

Table 1: Variables stored in database mean data files

Mean variable	symbol	units	2-D or 3-D
Surface temperature	tsurf	K	2-D
Surface pressure	ps	Pa	2-D
LW (thermal IR) radiative flux to surface	fluxsurf_lw	$W m^{-2}$	2-D
SW (solar) radiative flux to surface	fluxsurf_sw	$W m^{-2}$	2-D
LW (thermal IR) radiative flux to space	fluxtop_lw	$W m^{-2}$	2-D
SW (solar) radiative flux to space	fluxtop_sw	$W m^{-2}$	2-D
CO ₂ ice cover	co2ice	$kg m^{-2}$	2-D
Visible Dust optical depth at 610 Pa	tauref		2-D
Height of thermals in the PBL	zmax	m	2-D
Maximum thermals heat flux	hfmax	K.m/s	2-D
Vertical velocity scale in thermals	wstar	m/s	2-D
Water vapor column	col_h2ovapor	kg/m^2	2-D
Water ice column	col_h2oice	kg/m^2	2-D
H ₂ O ice cover (seasonal frost)	h2oice	$kg m^{-2}$	2-D
CO ₂ column	c_co2 ³	molecules/cm ²	2-D
CO column	c_co ³	molecules/cm ²	2-D
O column	c_o ³	molecules/cm ²	2-D
O ₂ column	c_o2 ³	molecules/cm ²	2-D
O ₃ column	c_o3 ³	molecules/cm ²	2-D
H column	c_h ³	molecules/cm ²	2-D
H ₂ column	c_h2 ³	molecules/cm ²	2-D
N ₂ column	c_n2 ³	molecules/cm ²	2-D
Ar column	c_ar ³	molecules/cm ²	2-D
He column	c_he ³	molecules/cm ²	2-D
Total Electronic Content (TEC)	c_elec	electrons/cm ²	2-D
Atmospheric density	rho	$kg m^{-3}$	3-D
Atmospheric temperature	temp	K	3-D
Zonal (East-West) wind	u	$m s^{-1}$	3-D
Meridional (North-South) wind	v	$m s^{-1}$	3-D
Vertical (up-down) wind	w	$m s^{-1}$	3-D
Water vapor mixing ratio	vmr_h2ovapor	mol/mol	3-D
Water ice mixing ratio	vmr_h2oice	mol/mol	3-D
CO ₂ volume mixing ratio	vmr_co2	mol/mol	3-D
CO volume mixing ratio	vmr_co	mol/mol	3-D
O volume mixing ratio	vmr_o	mol/mol	3-D
O ₂ volume mixing ratio	vmr_o2	mol/mol	3-D
O ₃ volume mixing ratio	vmr_o3	mol/mol	3-D
H volume mixing ratio	vmr_h	mol/mol	3-D
H ₂ volume mixing ratio	vmr_h2	mol/mol	3-D
N ₂ volume mixing ratio	vmr_n2	mol/mol	3-D
Ar volume mixing ratio	vmr_ar	mol/mol	3-D

³Note that the column is converted in $kg m^{-2}$ when output from the MCD

Table 1: Variables stored in database mean data files

He volume mixing ratio	vmr_he	mol/mol	3-D
Electron number density	vmr_elec	mol/mol	3-D
Dust mass mixing ratio	dustq	kg/kg	3-D
Dust effective radius	reffdust	m	3-D
Water ice effective radius	reffice	m	3-D

Day to day variabilities (RMS) Pressure-wise and/or altitude-wise	ARMS symbol	RMS symbol	units	2-D or 3-D
Surface temperature		rmstsurf	K	2-D
Surface pressure		rmsps	Pa	2-D
CO ₂ ice cover		rmsco2ice	kg m ⁻²	2-D
Dust optical depth		rmsdod		2-D
Atmospheric temperature	armstemp	rmstemp	K	3-D
Atmospheric density	armsrho	rmsrho	kg m ⁻³	3-D
Zonal (East-West) wind	armsu	rmsu	m s ⁻¹	3-D
Meridional (North-South) wind	armsv	rmsv	m s ⁻¹	3-D
Vertical (down-up) wind	armw	rmsw	m s ⁻¹	3-D
Atmospheric pressure	armspressure		Pa	3-D

Table 2: Variables stored in database standard deviation data files - lower atmosphere. For 3-D variables, the 'arms' prefix indicates an altitude-wise RMS and the 'rms' prefix a pressure-wise RMS.

Day to day variabilities (RMS) Pressure-wise and/or altitude-wise	ARMS symbol	RMS symbol	units	2-D or 3-D
Atmospheric temperature	armstemp	rmstemp	K	3-D
Atmospheric density	armsrho	rmsrho	kg m ⁻³	3-D
Zonal (East-West) wind	armsu	rmsu	m s ⁻¹	3-D
Meridional (North-South) wind	armsv	rmsv	m s ⁻¹	3-D
Vertical (down-up) wind	armsw	rmsw	m s ⁻¹	3-D
Atmospheric pressure	armspressure		Pa	3-D

Table 3: Variables stored in database standard deviation data files - thermosphere. For 3-D variables, the 'arms' prefix indicates an altitude-wise RMS and the 'rms' prefix a pressure-wise RMS.

The EOF datafiles (e_o) contain normalized, multi-dimensional EOFs of zonal wind, meridional wind, atmospheric temperature and surface pressure as well as some normalization factors, eigenvalues and principal component model coefficients. It is recommended that you use the software supplied to access and exploit the data in these files.

2.4 Database Grid Structure

2.4.1 Horizontal Structure

Variables in the database are stored on the grid on which they are obtained from the general circulation model (GCM) runs: a regular, equispaced horizontal 64 × 49 grid⁴ in East longitude × latitude.

⁴Technically, this grid is not exactly the computational grid: dynamical variables are in fact computed on a complementary staggered grid.

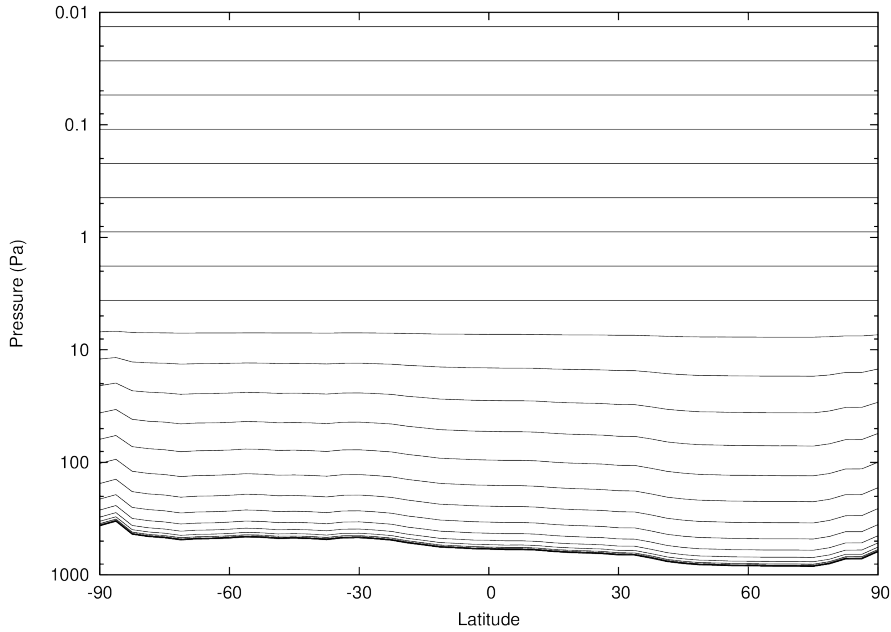


Figure 1: Illustration of the vertical hybrid coordinate system used to define MCD vertical levels. It follows the topography at low altitude and becomes equal to pressure in the free atmosphere. Note that not all levels are shown. The MCD vertical levels extend to much lower pressures, down to $P = 2.10^{-8}$ Pa for the last (49th) level.

Longitudes thus range from -180.0° to 174.375° in steps of 5.625° and latitudes from 90° to -90° in steps of 3.75° .

2.4.2 Vertical Structure

Variables in the database are stored on the same vertical grid on which they are computed. This vertical coordinate is a hybrid coordinate in which vertical levels l are at pressure P :

$$P(l) = aps(l) + bps(l) \times P_S \quad (1)$$

where P_S is surface pressure. Coefficients $aps(l)$ and $bps(l)$ are respectively hybrid pressure and hybrid sigma levels.

In its present form the database extends over 49 levels and variables in the datafiles are split between lower atmosphere ($l = 1, \dots, 30$) and thermospheric ($l = 31, \dots, 49$, for `thermo` datafiles). This is due to the fact that only the thermosphere is affected by solar EUV input, unlike the lower part of the atmosphere. In order to reconstruct a column of data, one must thus extract the first 30 levels from 'lower atmosphere' datafiles and obtain the following 19 from the corresponding 'thermosphere' datafiles.

Note that aps and bps are prescribed coefficients such that near the surface (small values of l) levels are essentially terrain-following sigma coordinates, whereas at high altitude (large values of l) the vertical levels are pressure levels, as shown in Figure 1. Values of coefficients aps and bps are given in the following table, along with corresponding pseudo-altitude which are the approximative heights above local surface of the corresponding layer (computed using a surface pressure of 610 Pa and a scale height of 10 km; it is thus a rough estimate and particularly inaccurate in the upper atmosphere above 80 km because it does not account for actual changes in temperatures and scale height there).

Layer	hybrid pressure level aps (Pa)	hybrid sigma level bps	Typical pressure (Pa)	pseudo-altitude above surface (km)
1	4.5543909E-03	0.9995446	609.7	0.0045
2	2.3923520E-02	0.9976096	608.5	0.0236
3	7.5913072E-02	0.9924263	605.4	0.0747
4	0.1893115	0.9811697	598.7	0.18
5	0.4006350	0.9603562	586.2	0.40
6	0.7515073	0.9262172	565.7	0.75
7	1.284045	0.8752495	535.1	1.30
8	2.027396	0.8054483	493.3	2.12
9	2.978001	0.7177855	440.8	3.24
10	4.089087	0.6165482	380.2	4.72
11	5.272429	0.5086969	315.5	6.59
12	6.415585	0.4023946	251.8	8.84
13	7.414103	0.3047343	193.3	11.49
14	8.194447	0.2204070	142.6	14.53
15	8.719654	0.1516246	101.2	17.96
16	8.985525	9.8466769E-02	69.1	21.78
17	9.009363	5.9486639E-02	45.3	26.00
18	8.812431	3.2389790E-02	28.6	30.61
19	8.386410	1.4656390E-02	17.3	35.61
20	7.516405	4.2412281E-03	10.1	41.00
21	5.462468	3.3150270E-04	5.66	46.79
22	3.055439	1.9820741E-11	3.05	52.96
23	1.589822	0.	1.59	59.5
24	0.8035691	0.	0.80	66.3
25	0.3999312	0.	0.40	73.3
26	0.1985999	0.	0.199	80.3
27	9.8621808E-02	0.	9.8621808E-02	87.
28	4.8974149E-02	0.	4.8974149E-02	94.
29	2.4319850E-02	0.	2.4319850E-02	101.
30	1.2076880E-02	0.	1.2076880E-02	108.
31	5.9971968E-03	0.	5.9971968E-03	115.
32	2.9781200E-03	0.	2.9781200E-03	122.
33	1.4788910E-03	0.	1.4788910E-03	129.
34	7.3439581E-04	0.	7.3439581E-04	136.
35	3.6469029E-04	0.	3.6469029E-04	143.
36	1.8109979E-04	0.	1.8109979E-04	150.
37	8.9931491E-05	0.	8.9931491E-05	157.
38	4.4658649E-05	0.	4.4658649E-05	164.
39	2.2176841E-05	0.	2.2176841E-05	171.
40	1.1012690E-05	0.	1.1012690E-05	178.
41	5.4687389E-06	0.	5.4687389E-06	185.
42	2.7156959E-06	0.	2.7156959E-06	192.
43	1.3485750E-06	0.	1.3485750E-06	199.
44	6.6968261E-07	0.	6.6968261E-07	206.
45	3.3255461E-07	0.	3.3255461E-07	213.
46	1.6514160E-07	0.	1.6514160E-07	220.
47	8.2006913E-08	0.	8.2006913E-08	227.
48	4.0723439E-08	0.	4.0723439E-08	234.
49	2.0222670E-08	0.	2.0222670E-08	241.

2.4.3 Temporal Structure

In order to store the seasonal behaviour of variables, data from the Global Climate Model was processed to be stored along 12 martian months. Each of these month is defined as spanning 30° in

Month number	Solar longitude range	Duration (in sols)
1	0 - 30	61
2	30 - 60	66
3	60 - 90	66
4	90 - 120	65
5	120 - 150	60
6	150 - 180	54
7	180 - 210	50
8	210 - 240	46
9	240 - 270	47
10	270 - 300	47
11	300 - 330	51
12	330 - 360	56

Table 5: Length of martian months. Note that a martian year is 668.6 sols (martian solar days) long and that a sol is 88775.245 seconds long; For convenience, the durations given above are rounded to be integer values.

solar longitude (months are thus “centered” on solar longitudes $L_s = 15^\circ, 45^\circ, \dots$). Due to the eccentricity of Mars’ orbit, martian months vary from 46 to 66 sols (martian solar days) long, as shown in Table 5.

Time evolution of variables on the scale of a sol is included in the datafiles where values at 12 times of day are stored. Martian hours are defined as being 1/24th of a sol. To avoid confusion, we do not use (or define) martian minutes or seconds: any martian time of day is always given as a fraction of a sol or in martian hours and decimal fractions thereof (e.g. $time = 18.5$ hours means 18 hours and a half).

The database reference time is Mars Universal Time (which is simply “prime meridian time”, i.e. the local time at 0° longitude) and data is stored every 2 martian hours, i.e. from 2 to 24 hours. Note that all times are expressed in True Solar Time (the sun is highest at noon) and not Mean Solar Time (see the description of the Equation Of Time in Appendix A).

The Local True Solar Time $LTST$ at a given East longitude lon (expressed in degrees) may easily be computed from the Local True Solar Time at longitude zero $LTST_0$ (i.e. Mars Universal Time) by the following formula:

$$LTST = LTST_0 + lon/15 \quad (2)$$

3 Dust Distribution and EUV Scenarios in the MCD

Combinations of dust and solar scenarios are provided because these are the two forcings that are highly variable from year to year.

- On the one hand, the solar conditions describe variations in the Extreme UV input which control the heating of the atmosphere above 120 km, which typically varies on a 11 years cycle. Depending on the scenarios, either fixed solar maximum average and/or minimum conditions or realistic (evolving daily) solar conditions are used.
- On the other hand, the major factor which governs the variability in the Martian atmosphere is the amount and distribution of suspended dust. Because of this variability, and since even for a given year the details of the dust distribution and optical properties can be uncertain, multi-annual model integrations were carried out for the database assuming various “dust scenarios”, i.e. prescribing various amount of airborne dust in the simulated atmosphere.

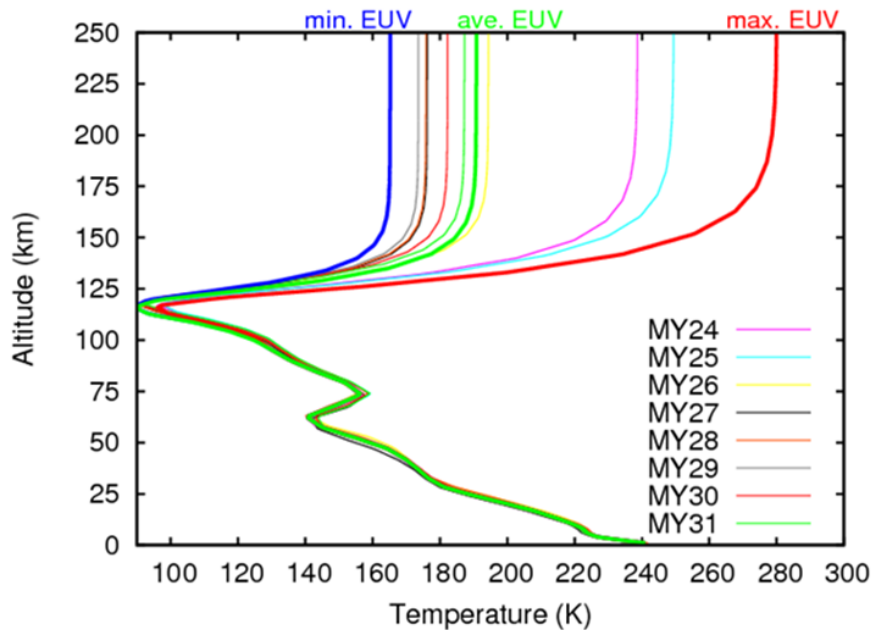


Figure 2: Illustration of temperature profiles at a given location provided by the GCM (with the same “clim” dust scenario) with the Extreme Ultraviolet (EUV) fluxes corresponding to the daily evolution observed during Martian Years 24-31 as well as the solar EUV minimum (min), average (ave) and maximum (max) scenarios.

How these dust and EUV scenarios are taken into account is detailed in the following subsections.

3.1 The EUV Scenarios

The radiative output of the Sun is known to vary at different timescales: for example, due to the solar flares (timescale of minutes to hours), to the solar rotation (27 days) or to the magnetic cycle of the Sun (11 years, the so-called solar cycle). This last variability, first detected counting the number of sunspots, is more important in the UV (than in the visible) region of the solar spectrum, as a variability of about a factor 2 in the total EUV irradiance (below 120 nm) with the solar cycle is found. Although the UV spectral region represents a small contribution to the total solar energy, the UV radiation is the major heating source of the Martian upper atmosphere (above about 120 km). So, its variability has a strong impact over the thermospheric temperatures.

The EUV flux is represented in two manners in the MCD.

- In some of the MCD simulations, the EUV flux is set to constant values chosen to provide an estimation of the average and extreme (minimum and maximum) fluxes. The “**Solar maximum**” scenario corresponds to conditions when the solar cycle is at its maximum activity (value for E10.7⁵ at Earth around 320) and the UV emission is highest. For such conditions, a rise in temperatures in the thermosphere, induced by a more intense UV heating, is expected (and obtained). On the opposite, the “**Solar minimum**” scenario is appropriate for conditions when the sun is at its minimum activity (approximate value of E10.7 at Earth around 80). In this case, UV emission is low, so a lower temperature due to a lower UV heating is expected. The “**Solar average**” scenario is an intermediate situation between maximum and minimum

⁵E10.7 is a proxy for the integrated extreme ultraviolet flux from 1 to 105 nm expressed in the same unit than the canonic F10.7 index (full-disc solar emission at the 10.7 cm wavelength, expressed in units of $10^{-22} \text{ W m}^{-2} \text{ hz}^{-1}$) originally measured by Earth-based radio-observatory when no solar spectral EUV fluxes is available.

solar activity (approximate value for E10.7 at Earth 140) Figure 2 displays mean temperature profiles corresponding to the three EUV scenarios.

- Simulations were also performed with a realistically (daily) evolving EUV input, taken from available E10.7 measurements, over the Martian years 24-31. Figure 2 also displays the mean thermospheric profiles corresponding to these 8 martian years .

3.2 The Dust Scenarios

This section outlines the dust distribution scenarios used for the GCM integrations which make up the Mars Climate Database.

3.2.1 Parametrization of dust vertical distribution and particle size variations

In our simulations, at every location and time, the total dust column optical depth is prescribed to match the available observations. However, the dust vertical distribution and the dust particle size is computed online by the global climate model. This is detailed in the joined scientific paper (file `dust_distribution_jgr2011.pdf`) by Madeleine et al. (2011). In summary:

1. **Dust vertical distribution:** In the global climate model, the dust vertical distribution is now estimated by following idealized dust-like tracers. The dust distribution is controlled by the balance between general circulation and gravitational sedimentation.
2. **3D variation of dust particle radii.** By transporting two moments of the dust fields (mass mixing ratio and number mixing ratio), the above scheme is used to simulate the gravitational segregation of larger dust particles and realistically simulate the decrease of dust effective radius in the vertical.
3. **Dust Single Scattering Properties.** We now use improved indexes of refraction provided by M. Wolff based on a variety of orbital and in-situ observations, and compute the single scattering properties of various dust size distributions using T-matrix theories following Wolff et al. *J. Geophys. Res.*, 112, E08S16 (2009). We have found that these properties allow for the first time to reconcile the observed amount of dust in the atmosphere with the temperatures observed simultaneously.
4. **Impact of dust scavenging by water ice condensation.** The condensation of ice particles is now taken into account to physically increase the sedimentation rate of the dust particles on which water ice has condensed.

3.2.2 Prescribed dust column optical depth variations

1. The “**Climatology**” (**clim**) scenario is derived from the available observations of dust from multiple years between $L_s \sim 105^\circ$ in Martian year ⁶ 24, 26, 27, 29, 30, 31 (years without global planet-encircling dust storms).

For this purpose, we carefully gathered and combined all available observations for each available year to reconstruct the dust field and its evolution as described in the joined paper (file `dust_climatology_icarus2015.pdf`) by Montabone et al. (2015). In summary we used observations of the Martian atmosphere from April 1999 to July 2013 by different orbiting instruments: the Thermal Emission Spectrometer (TES) on board Mars Global Surveyor, the Thermal Emission Imaging System (THEMIS) on board Mars Odyssey, and the Mars Climate Sounder (MCS) on board Mars Reconnaissance Orbiter (MRO). The data have been gridded and interpolated using a kriging method.

⁶This widely used numbering of martian years follows the calendar proposed by R. Todd Clancy (Clancy et al., *Journal of Geophys. Res.* 105, p 9553, 2000) which begins on April 11, 1955 ($L_s=0^\circ$)

Figure 3 present the seasonal evolution of the zonal mean dust opacity for the 8 available Martian years.

To make the “climatic” simulation and estimate the reference simulations, we performed several sets of simulations:

- Mean atmospheric fields and their day-to-day variability are retrieved from a simulation performed using an averaged “climatic” dust scenario obtained by using the geometric mean the dust column optical depth from Martian years 24, 26, 27, 29, 30, 31 (years without global dust storm).
- As detailed in Section 5.2.4, the Large-scale variability perturbations provided with the clim scenario include a realistic interannual variability obtained by retrieving statistics from 6 independent simulations performed using Martian years 24, 26, 27, 29, 30, 31 dust scenarios.

This “Climatology” scenario is provided with 3 solar EUV conditions: solar min, solar ave, solar max.

2. The **cold scenario** corresponds to an extremely clear atmosphere (“Low dust scenario”). At a given seasonal date (Ls) and location, the dust opacity is set to be the minimum observed over Mars years 24-31, further decreased by 50%, topped with a solar minimum thermosphere (figure4). In addition, in these simulations the **radiative effects of water ice clouds is not taken into account** (clouds usually tend to warm the atmosphere)
3. The **warm scenario** corresponds to “dusty atmosphere” conditions, but nonetheless non-global dust storm conditions. The dust opacity at a given location and seasonal date (Ls) is set to the maximum observed over the seven Mars years (MY24-MY31), except during the MY25 and MY28 global dust storms, further increased by 50%, topped with a solar maximum thermosphere (figure5).
4. The **dust storm scenario** represents Mars during extreme global dust storms. The dust opacity is set to $\tau = 5$ at all times and over the whole planet. Moreover the dust optical properties are for this case set to represent “darker dust” than nominal (in practice for these runs, dust properties from Ockert-Bell et al. (*J. Geophys. Res.*, 102, 9039-9050, 1997) were used, rather than the more recent properties from Wolff et al. *J. Geophys. Res.*, 112, E08S16, 2009) used for all other MCD simulations).

This scenario is only provided for when such storms are likely to happen, during northern fall and winter (Ls=180-360), but with 3 cases of solar EUV inputs: solar min, solar ave, solar max.

Because the most intense phases of global dust storms (i.e. with visible opacities larger than 3) only last for a few weeks, to ensure a realistic behaviour of the water and CO₂ cycle (and the associated pressure cycle), the dust storm simulations are started from initial states retrieved from the reference “clim” scenario at the beginning of each Martian months. In other words, the MCD dust storm scenario provides statistics on a Martian atmosphere experiencing a typical intense Ls=30° long dust storm. This scenario remains extreme because the atmosphere react very quickly to the onset of such an intense dust storm. Nevertheless this allows to capture in the statistics the variability induced by the onset of the dust storms.

5. The **Mars years scenarios**, MY24, MY25, MY26, MY27, MY28, MY29, MY30, MY31 and MY32. As already mentionned, we have access to the daily evolution of Martian atmospheric dust loading as well as to the daily evolution of the EUV received at Mars from the Sun for Mars years 24 to 31. The associated outputs correspond to our best representation of the Martian climate over these specific years.

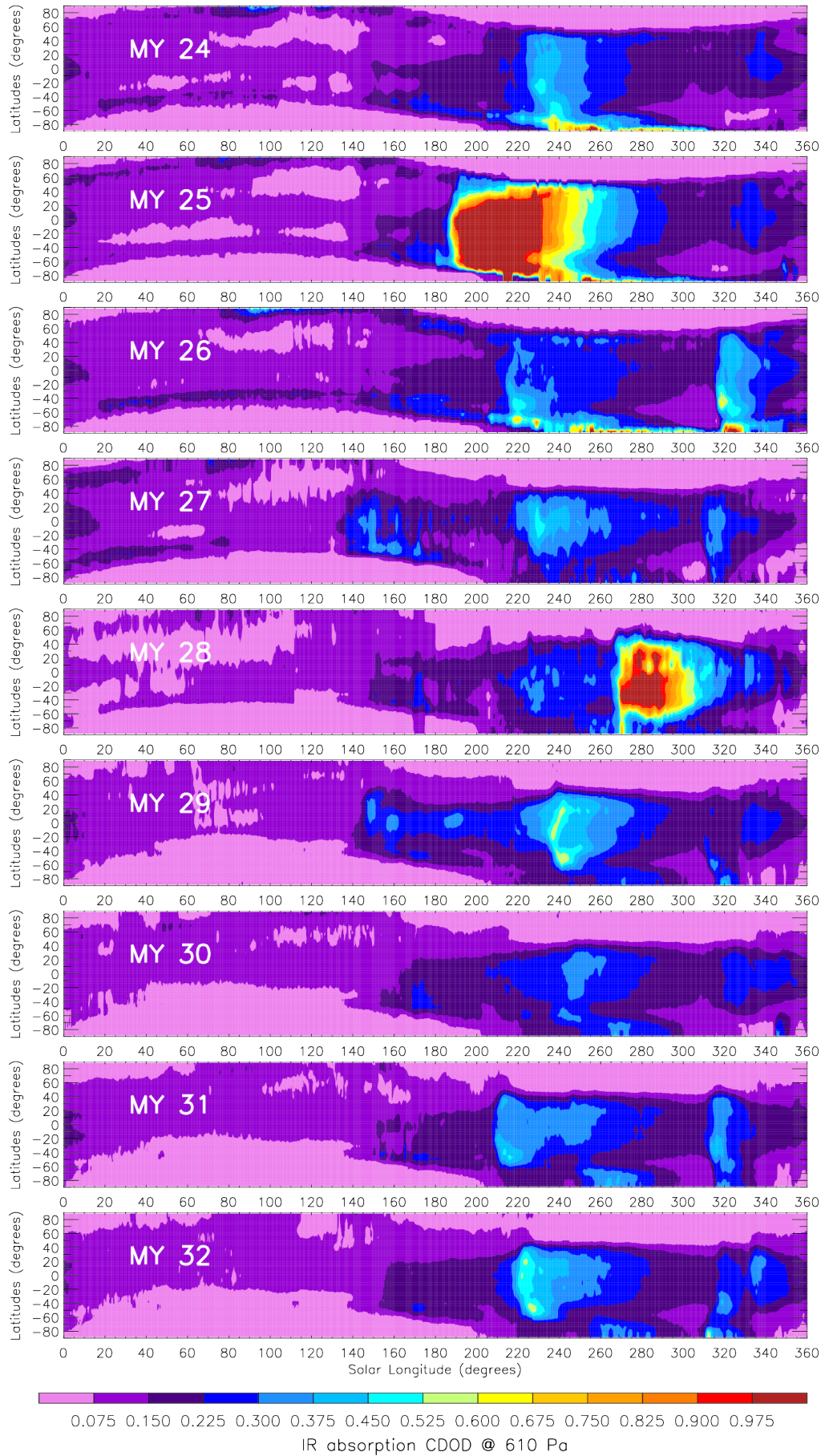


Figure 3: Dust scenarios derived from available observations and used as inputs to compute the database simulations. This figure shows the zonal means of dust absorption optical depth at infrared wavelength $9.3 \mu\text{m}$ (referred to pressure level 610 Pa) as a function of latitude and solar longitude for all 9 available Martian years. These infrared dust column opacities are converted to extinction visible dust opacities by multiplying them by a factor of 2.6.

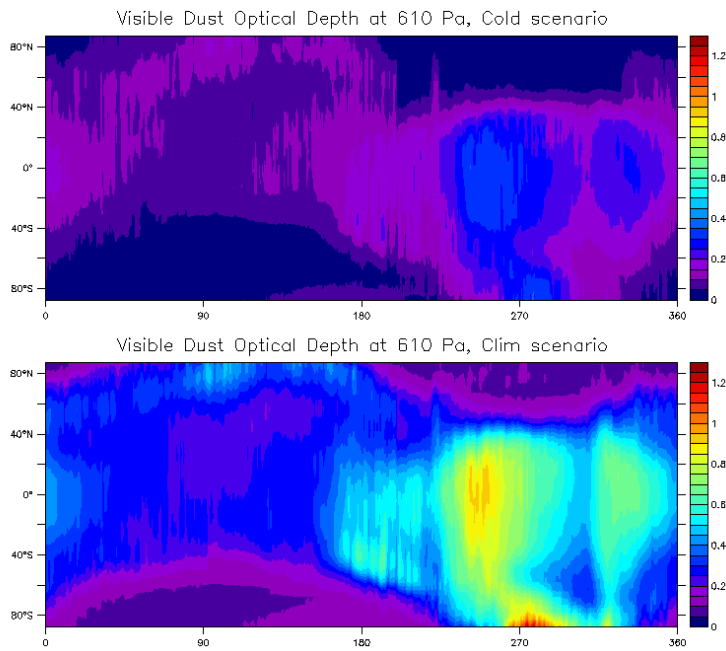


Figure 4: Seasonal evolution of the visible dust optical depth for the “cold” scenario (top plot), along with the reference “clim” scenario (bottom plot) for comparison (the same color scale is used for both plots).

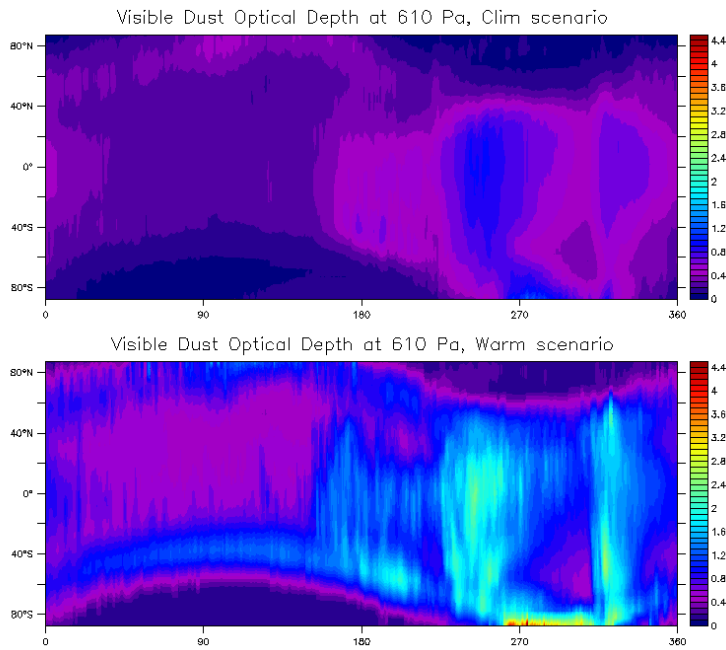


Figure 5: Seasonal evolution of the dust visible optical depth for the “warm” scenario (bottom plot), along with the “clim” scenario (top plot) for comparison (the same color scale is used for both plots).

4 Technical description of Methods Used to Retrieve Data from the MCD

4.1 Temporal Interpolations

Once the time of year and of day at which data is requested is known (see Appendix A for details on how these can be computed for a given Julian date), linear interpolation between datasets of encompassing months along with linear interpolation between encompassing stored martian hours are used to evaluate data on the GCM grid.

4.2 Spatial Interpolations

4.2.1 Horizontal Interpolation

To compute the values of variables at a given location (which is not on the GCM grid), one needs to first build a virtual column of data along what would have been GCM levels. This profile is obtained by horizontal interpolation of encompassing grid values. To be specific, values of variables are obtained from encompassing grid values using bilinear interpolation, except for density ρ (and similar bi-products such as associated RMS or surface pressure), which is obtained using bilinear interpolation of $\log(\rho)$.

4.2.2 Vertical Interpolation

In order to compute the value of meteorological variables at a given height (or pressure), one must first identify the altitudes (and pressure) of the vertical levels of the profile. This is done by integrating the hydrostatic equation over the column:

$$\frac{\partial P}{\partial z} = -g \cdot \rho = -g \cdot \frac{P}{R \cdot T} \quad (3)$$

from which the relation between an increment in altitude δz and average (over δz), gas constant R_m , atmospheric temperature $T_m = \delta T / \log(\delta T)$, and \log pressure increment $\delta \log P$ can be derived:

$$\delta z = -\frac{R_m}{g_m} \cdot T_m \cdot \delta \log P \quad (4)$$

This relation can be used to compute the altitudes of all the levels of a profile for which pressure $P(l)$ (or equivalently sigma levels $\sigma(l) = P(l)/P_S$, where P_S is surface pressure), atmospheric temperature $T(l)$ as well as gas constant $R(l)$ at all l levels are known. Moreover, as the database extends to high altitudes, it must also taken into account that gravity g varies as the inverse square of the distance to the center of the planet, i.e. that gravity at altitude z can be approximated as $g(z) = g_0 \cdot a_0^2 / (a_0 + z)^2$, where z is the altitude above the areoid a_0 , and $g_0 = 3.7257964 \text{ m/s}^2$ is the gravity at $a_0 = 3.39610^6 \text{ m}$.

The altitude of the first atmospheric layer is thus obtained using:

- Gravity $g(l = 1)$ is approximated to be that at the surface (of known orography, i.e. altitude above areoid, h):

$$g(l = 1) = g_0 \cdot a_0^2 / (a_0 + h)^2$$

- The altitude of the first layer is then simply

$$z(l = 1) = -[R(l = 1)/g(l = 1)] \cdot T(l = 1) \cdot \log(\sigma(l = 1))$$

From there, the altitudes of layers are recursively determined; i.e. for layer $l + 1$:

- Approximate $g(l + 1)$ using the altitude $z(l)$ of previous layer:

$$g(l + 1) = g_0 \cdot a_0^2 / (a_0 + h + z(l))^2$$

- Compute altitude of level $l + 1$:

$$z(l + 1) = z(l) - [R(l + 1)/g(l + 1)] \cdot T(l + 1) \cdot \log[\sigma(l + 1)/\sigma(l)]$$

Once the altitudes $z(l)$ of layers are known, then the value of a variable X at a given altitude above the surface z_s may be obtained from linear interpolation of values at encompassing grid points. For variables which are, to first order, exponentially distributed in altitude (e.g. pressure, density and associated variables) then the interpolation must naturally be performed on the logarithm of these values.

4.2.3 Specific Treatments of Vertical Interpolation

Interpolation, as explained above, is feasible when the altitude (or pressure) at which the value of a variable is sought falls in the range of the MCD grid. In the more extreme cases, either above the topmost atmospheric layer or below the lowest one, different approaches must be used. These are detailed here.

Above the MCD Topmost Layer

If above the MCD topmost layer $l = L$, then the concentration of component j of the neutral atmosphere at the altitude z_s is:

$$n_j(z_s) = n_j(L) \frac{T(L)}{T(z_s)} \exp\left\{-\int_{z(L)}^{z_s} \frac{g(z)}{R_j T(z)} dz\right\} \quad (5)$$

where n_j and R_j are the concentration and gas constant of specie j (in $\text{m}^2 \text{s}^{-2} \text{K}^{-1}$). This results from the fact that, in the upper thermosphere and exosphere the collision rate of molecules and atoms is so small that each species tend to have its own scale height.

Assuming that the gravity decreases inversely to the square of planetocentric radial coordinate as:

$$g(z) = g(L) \left(\frac{a_0 + h + z(L)}{a_0 + h + z}\right)^2 \quad (6)$$

Neglecting by the variation of neutral temperature with altitude $T(z > z(L)) \cong T(L)$ the pressure $P(z_s)$ at altitude z_s is:

$$P(z_s) = \sum_j P_j(L) \exp\left\{-\frac{g(L)}{R_j T(L)} \frac{(a_0 + h + z(L))(z_s - z(L))}{a_0 + h + z_s}\right\} \quad (7)$$

With $P_j(L)$ the partial pressure of specie j in the top layer of the model. When the vertical coordinate is requested in pressure units the conversion into meters is implemented numerically by the bisection method with 5% precision. Therefore, small discrepancies between cases with vertical coordinate defined in [Pa] and [m] may happen.

The density, pressure and volume mixing ratios of neutral species are computed according to these relations but all other variables (e.g. winds) are not extrapolated and are assumed to remain constant above the topmost layer.

Below the Lowest MCD Layer

When below the lowest MCD layer $l = 1$ (which typically lies at 5 m above the surface, see table in Section 2.4.2), then pressure $P(z_s)$ at altitude z_s above the surface is computed using a hydrostatic vertical profile, i.e.:

$$P(z_s) = P(1) \exp [(z(1) - z_s) \cdot g(z_s) / (R(1) \cdot T(1))]$$

where $P(1)$, $R(1)$ and $T(1)$ are the pressure, gas constant and temperature at the first layer, $z(1)$ its altitude and $g(z_s)$ is gravity at altitude z_s . This formulation enables recovery of the value of surface pressure P_s when $z_s = 0$.

Density ρ , as well as the RMS of these two variables, are treated similarly.

Other variables (except horizontal winds and atmospheric temperature) are not extrapolated and are taken to be constant from the middle of the first atmospheric level down to the surface.

Near Surface Atmospheric Temperature and winds

Below the lowest MCD layer, temperature and winds are estimated using the Monin-Obukhov similarity theory which take into account the stability of the atmosphere (via its Richardson number), the sub-grid scale gustiness and the roughness length z_0 .

The values of the horizontal winds are set to zero below the roughness length z_0 .

5 Variability Models in the MCD

5.1 Day-to-Day RMS of Variables

The MCD provides the day-to-day variability of variables computed from the outputs of the Global Circulation Model (GCM). This day-to-day RMS of variable X is computed over each month as:

$$RMS(X) = \sqrt{\frac{1}{N} \sum_1^N (\langle X \rangle_{1 \text{ sol}} - \langle X \rangle_{10 \text{ sols}})^2} \quad (8)$$

where N is the number of samples from the time-series output of variable X over the month and $\langle X \rangle_{1 \text{ sol}}$ and $\langle X \rangle_{10 \text{ sols}}$ respectively denote running averaged values of X over a sol and 10 sols.

The RMS thus obtained represents the variability of a variable from one day to the next, at a given time of the day, regardless of the general drift over the month (removed by taking into account the deviation of diurnal values to 10-day averages, i.e. long term trends, in the computation of the RMS).

It is important to note that the RMS values obtained from the GCM outputs are computed on the GCM grid and that since the vertical coordinate is essentially (see Section 2.4.2) a pressure coordinate, the obtained RMS values are evaluated at constant pressure.

Apart from this pressure-wise RMS, the MCD now also provides altitude-wise RMS, which is computed in the same way, but on time series of GCM outputs which have been interpolated on a fixed altitude vertical coordinate grid. For some variables, which are dependent on pressure, e.g. density, the difference between pressure-wise and altitude-wise RMS can be quite significant.

5.2 The Large-Scale Variability Model

In the MCD, data are stored in 12 monthly bins and at 12 local times of day. Although this captures the main seasonal and diurnal components of variability, any intra-month or day-to-day (synoptic) variations are averaged out. Thus there is a need to simulate this variability, especially if the user

wishes to produce an ensemble of realizations of a variable at a particular seasonal date and local time of day which covers a realistic range of variability.

For this purpose, we store the 3D variability of pressure, temperature and winds using Empirical Orthogonal Functions (EOFs) over the different simulated years.

5.2.1 Calculation of EOFs and PCs

Consider a time series of longitude-pressure vectors of zonal wind, $u(\phi, p, t)$, meridional wind, $v(\phi, p, t)$, temperature, $T(\phi, p, t)$ and surface pressure $p^*(\phi, t)$ at M discrete time points and on L spatial points. We form a time series of vectors $\mathbf{D}(t)$, where

$$\mathbf{D}(t) = (\hat{u}(\phi, p, t), \hat{v}(\phi, p, t), \hat{T}(\phi, p, t), \hat{p}^*(\phi, t)) \quad (9)$$

and the hat $\hat{\cdot}$ denotes a removal of the series mean and normalization of variance operator,

$$\bar{u} = \frac{1}{ML} \sum_{m=1}^M \sum_{l=1}^L u_{ml} \quad (10)$$

$$\hat{u}_{ml} = \frac{u_{ml} - \bar{u}}{\sqrt{\frac{1}{ML} \sum_{m=1}^M \sum_{l=1}^L (u_{ml} - \bar{u})^2}} \quad (11)$$

where the m denotes time and the l denotes spatial point. Hence, with this normalization, the variance of the entire time series of $\mathbf{D}(t)$ is unity.

We then form the $(N \times N)$ covariance matrix, \mathbf{C} , such that

$$\mathbf{C} = \frac{1}{N} \mathbf{D} \mathbf{D}^T \quad (12)$$

where $N = (\text{number of horizontal points}) \times (3 \times \text{number of vertical points} + 1)$, \mathbf{D} is the $(N \times M)$ matrix whose rows are the vectors $\mathbf{D}(t)$ and the superscript T indicates the transpose.

The matrix \mathbf{C} is real symmetric and we can find the eigenvectors and eigenvalues and order them in decreasing eigenvalue magnitude. We note that if \mathbf{E}_i is the i th eigenvector then

$$|\mathbf{E}_i| = 1 \quad (13)$$

where $|\cdot|$ is the Euclidean Norm, and

$$\sum_{i=1}^N \lambda_i = 1 \quad (14)$$

where λ_i is the i th eigenvalue.

The i th principal component (PC) at time m , p_{mi} is defined as

$$p_{mi} = \sum_{n=1}^N D_{mn} E_{ni} = \mathbf{D} \cdot \mathbf{E}_i \quad (15)$$

and we note the result

$$\frac{1}{MN} \sum_{m=1}^M (p_{mi})^2 = \lambda_i \quad (16)$$

Each principal component has 669 values during one year (one per day).

5.2.2 Storage of variability with EOFs

As described above using PCs and their smoothed version provides a mean to store variability.

In practice, any state vector $V(\text{lon}, \text{lat}, \text{alt}, \text{time})$ can be decomposed as:

$$V(\text{lon}, \text{lat}, \text{alt}, \text{time}) = AVE(\text{lon}, \text{lat}, \text{alt}) + NORM(\text{lat}) \sum_i PC_i(\text{time}) \times EOF_i(\text{lat}, \text{lon}, \text{alt})$$

Where $AVE(\text{lon}, \text{lat}, \text{alt}, \text{time})$ is simply an average over the whole time series, $NORM(\text{lat})$ is a normalization factor and PC_i are the Principal components and the EOF_i the empirical orthogonal functions (note that these are function of spatial coordinates only).

By design the individual PC_i and EOF_i are ordered from the most “most significant” (contains the most information) to the “least significant” (contains the less information), so that truncating the series and keeping the N first EOFs will suffice to reconstruct the original signal. Therefore **this method allows to store several years of meteorological variability without having to store the huge amount of data initially produced by the model**. Nevertheless, to further limit the size of the final dataset (and also limit the size of the eigensystem to solve) the retained dataset consists of:

- Atmospheric temperature, zonal wind, meridional wind and surface pressure variables
- Fields sub-sampled on a reduced 32x24 longitude x latitude grid (half of the computational GCM 64x48 grid; but twice more than what had been used for MCDv4.3, where the reduced grid was 16x12), and for three-dimensional quantities, on all 50 vertical levels.
- A time sampling of one data point per day, which is sufficient to reconstruct a day-to-day variability (note that the daily evolution of variables is, like the seasonal monthly evolution, already include in the MCD datasets).
- Overall, this means that a single EOF contains $32 \times 24 \times (3 \times 50 + 1) = 115968$ elements, hence the need to retain as few as possible.

Concerning the number N of EOFs suitable to retain to be able to realistically represent the original signal and its inherent variability, it is quite straightforward to test, by direct comparison between the original signal and truncated reconstructions, which value of N is sufficient. Our tests have shown that N=200 is a reasonable choice (see e.g. figure 7).

5.2.3 Reconstructing a realistic variability

Rather than reconstructing the original signal, our goal is to the original variability to recreate a realistic one (in space and time). In order to do that, one has to separate the high frequency component (ie the day-to-day variability) from the low frequency seasonal evolution. Using the fact that the temporal behavior of the decomposition is fully contained in the principal components PC_i , it is straightforward to build an alternative set of principal components which are a smoothed version (i.e. computed from the PC_i using a moving averaging windows of 30 sols) of the latter. A smoothed version of the signal, $V_{sm}(\text{lon}, \text{lat}, \text{alt}, \text{time})$ is then simply obtained as:

$$V_{sm}(\text{lon}, \text{lat}, \text{alt}, \text{time}) = AVE(\text{lon}, \text{lat}, \text{alt}) + NORM(\text{lat}) \sum_i PC_{sm\ i}(\text{time}) \times EOF_i(\text{lat}, \text{lon}, \text{alt})$$

By combining reconstructions using PC_i and $PC_{sm\ i}$ one can extract the day-to-day variations from the original signal. Similarly, one can build a new set of principal components which combine the information contained in the smoothed reconstruction and to which is added the high frequency behavior from a different (e.g. within nearby sols) instant. In practice this means that after having randomly chosen a time shift $dtime$ (which can range from -15 sols to 15 sols), a new set of principal components $PC_{new\ i}$ is generated for all times:

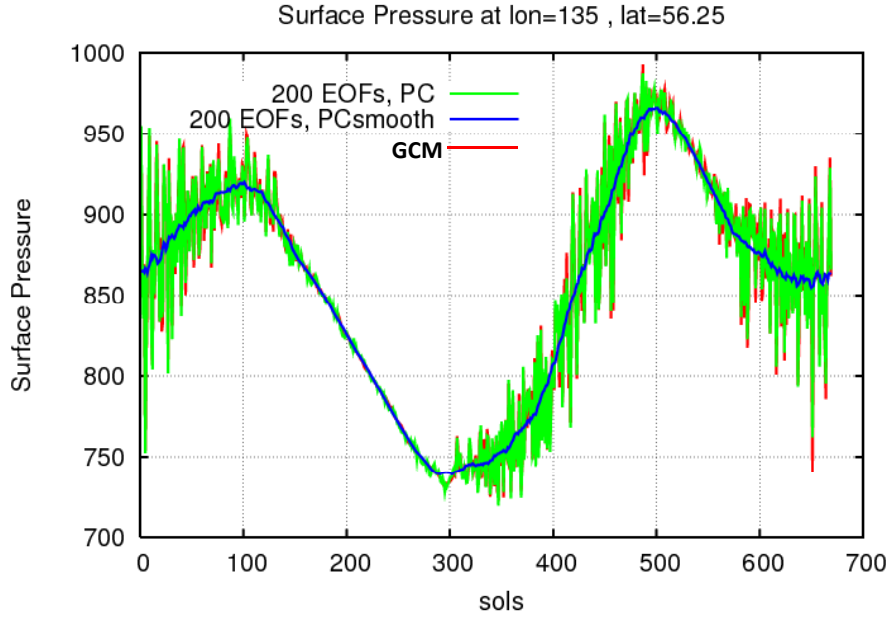


Figure 6: Example of the reconstruction of a signal (here surface pressure at a given node) with one data point per day, over one Mars year. The original signal simulated by the GCM (red) is compared to the MCD reconstruction (green) using 200 EOFs along with a reconstruction (blue) using the smoothed principal components $PC_{sm\ i}$ with which only the mean seasonal behavior is obtained.

$$PC_{new\ i}(\text{time}) = PC_{sm\ i}(\text{time}) + [PC_i(\text{time}+\text{dtime}) - PC_{sm\ i}(\text{time}+\text{dtime})]$$

And the perturbed series $V_{new}(\text{lon}, \text{lat}, \text{alt}, \text{time})$ is then reconstructed as:

$$V_{new}(\text{lon}, \text{lat}, \text{alt}, \text{time}) = AVE(\text{lon}, \text{lat}, \text{alt}) + NORM(\text{lat}) \sum_i PC_{new\ i}(\text{time}) \times EOF_i(\text{lat}, \text{lon}, \text{alt})$$

The key point in this procedure is that by construction the spatio-temporal coherence of transient phenomena is preserved, and that the true internal variability of the original signal is thus preserved and reproduced.

This is illustrated in figure 6 with a direct comparison, as well as in figure 7 where this time the RMS day-to-day variability of the reconstructed signal (as computed for each of the 12 Martian months, in the same way as is done in the MCD) is checked.

5.2.4 Reconstructing the inter-annual variability of the Martian atmosphere

As mentioned above, the “mean” scenario which reflects the climatological state of the atmosphere for regular Martian years is obtained as an ensemble average of 6 simulations using dust forcings corresponding to MY24, MY26, MY27, MY29, MY30 and MY31. From each of these simulations, an EOF decomposition has been obtained. The improved “large scale perturbation scheme” of MCDv5, when used with the “mean” scenario, uses all these sets to generate perturbed states. Repeated use of this “large scale perturbations scheme” thus give access to all the transient behaviors present in the simulations for the different Mars year, and thus offers the means to investigate the multi-annual variability of the system (figure 8).

In practice, the user doesn’t choose which EOF set is used to generate the perturbed state; switching from one EOF set to another when a new perturbation seed is provided by the user is done randomly (using that very same perturbation seed) by the MCD software

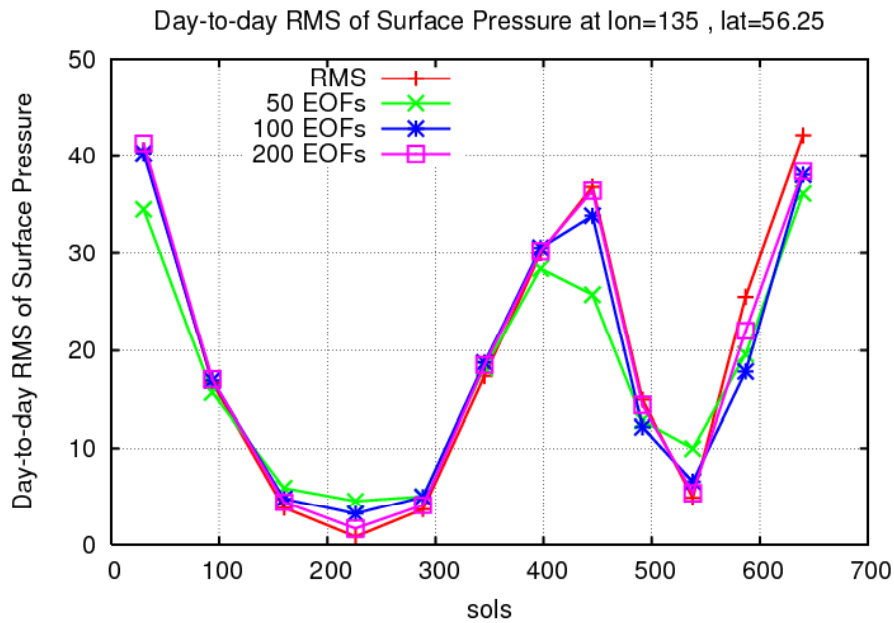


Figure 7: Example of day-to-day variability of surface pressure, computed for each of the twelve martian months, using perturbed series from the large scale perturbation model. RMS values for the original GCM series (corresponding to data at lon=135 E and lat=56.25 N, close to VL2 landing site) are also displayed for comparison, along with the RMS values that are obtained using 50, 100 and 200 EOFs..

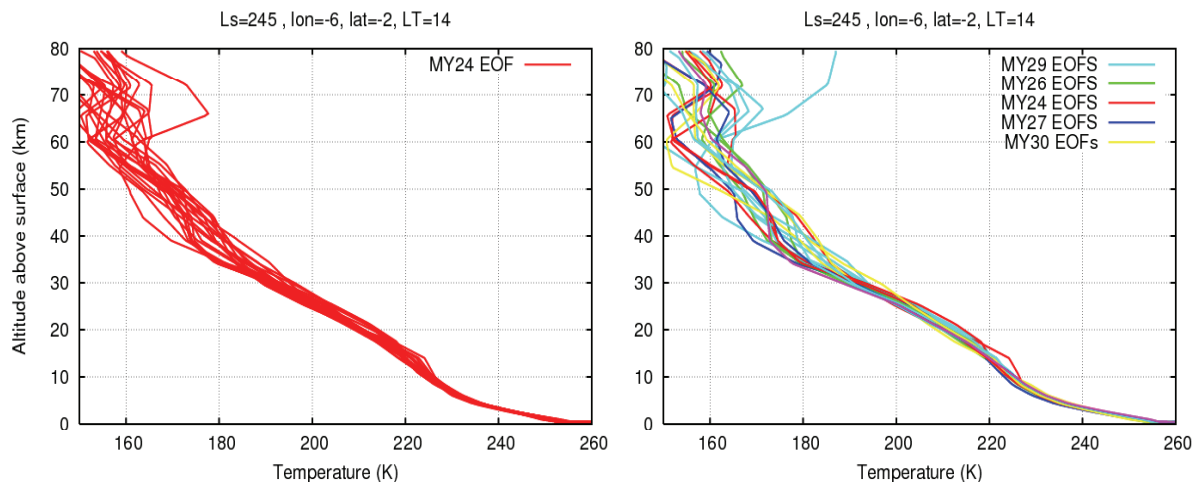


Figure 8: Illustration of the use of the MCDv5 “large scales perturbation scheme”. Left plot: Using only the 1 year “climatology” EOFs to generate perturbed states. Right plot: using all EOF sets; note that the color codes indicate from which EOF set the perturbation was reconstructed from, but that in practice the user does not choose which EOF set is used.

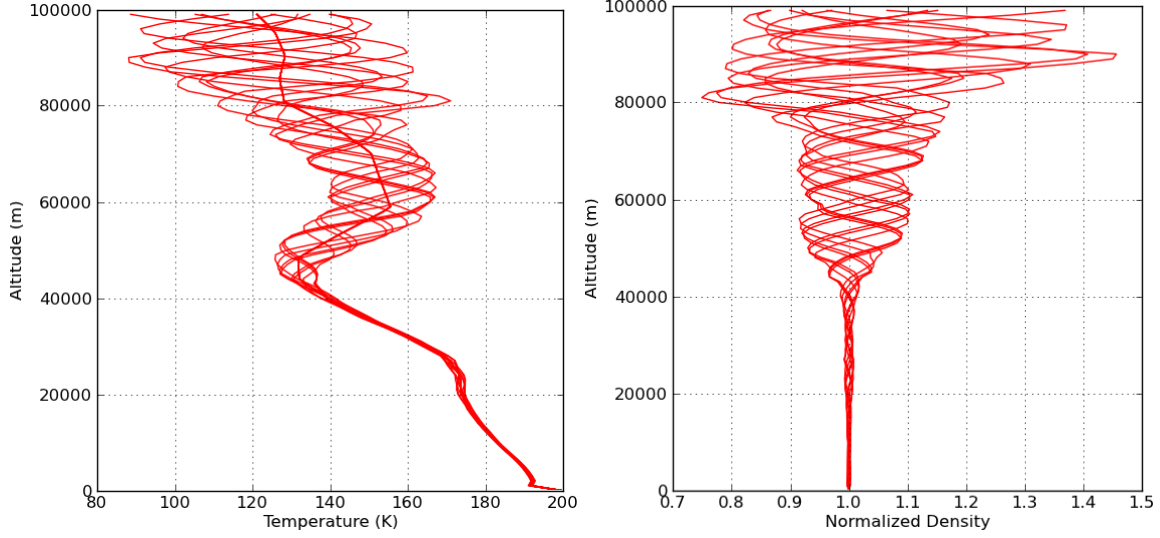


Figure 9: A series of ten perturbations, all with the same wavelength (16 km), generated by the small scale variability model added to mean profiles of temperature and density from the MCD on a vertical trajectory. Left plot: Atmospheric temperatures (including unperturbed profile). Right plot: density deviations (i.e. perturbed over unperturbed density ratios). Profiles obtained at longitude 230° East, latitude 30° South, Solar Longitude $L_s=73^\circ$ and a local time of 10 hours.

5.3 The Small-Scale Variability Model

The small-scale variability model simulates perturbations of density, temperature and wind due to the upward propagation of small-scale gravity waves. The model is based on the parameterization scheme used in the numerical models that simulated the data in the database (Forget et al., *J. Geophys. Res.* 104, 24,155-24,176, 1999)

The surface stress exerted by a vertically-propagating, stationary gravity wave can be written

$$\tau_0 = \kappa \rho_0 N_0 |\mathbf{v}_0| \sigma_0^2 \quad (17)$$

where κ is a characteristic gravity wave horizontal wave number, ρ_0 is the surface density, N_0 is the surface Brunt Väisälä frequency, \mathbf{v}_0 is the surface vector wind and σ_0 is a measure of the orographic variance. In this case we choose the model sub-grid scale topographic variance. The surface stress can be related to the gravity wave vertical isentropic displacement, δh , by

$$\tau_0 = \kappa \rho_0 N_0 |\mathbf{v}_0| \delta h^2. \quad (18)$$

We then assume that the stress, τ , above the surface is equal to that at the surface. This leads to an expression for the wave displacement δh , at height z ,

$$\delta h = \sqrt{\frac{\rho_0 N_0 |\mathbf{v}_0| \sigma_0^2}{\rho N |\mathbf{v}|}} \quad (19)$$

where ρ , N and \mathbf{v} are the density, Brunt Väisälä frequency and wind vector at height z .

The gravity wave perturbation to a meteorological variable is calculated by considering vertical displacements of the form

$$\delta z = \delta h \sin \left(\frac{2\pi z}{\lambda} + \frac{2\pi Dist}{\lambda_{Dist}} + \phi_0 \right) \quad (20)$$

where λ is a characteristic vertical wavelength for the gravity wave, λ_{Dist} is the horizontal wavelength, such as $\lambda_{Dist} = 10 \times \lambda$, and ϕ_0 is a randomly generated surface phase angle. A set of points

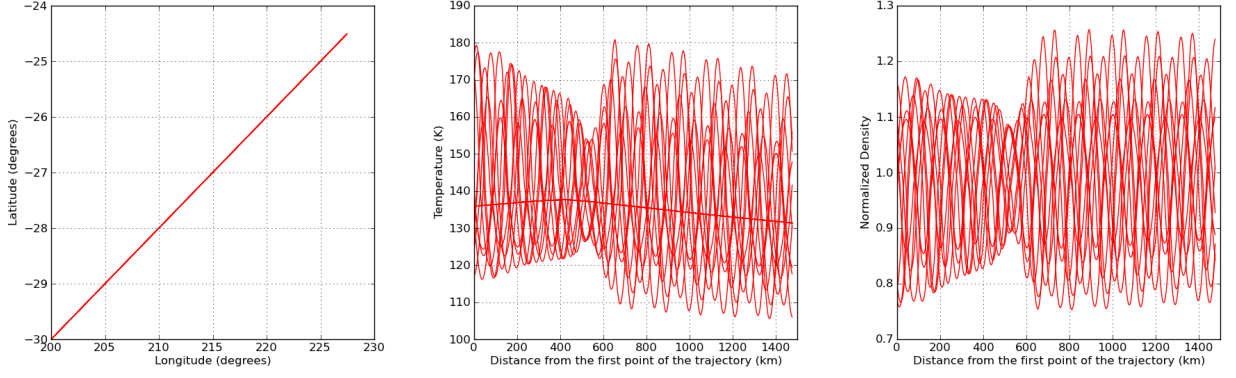


Figure 10: A series of ten perturbations, all with the same wavelength (16 km), generated by the small scale variability model added to mean profiles of temperature and density from the MCD with the example of a horizontal displacement. From left to right plot: depiction of the horizontal displacement along Latitude and Longitude; Atmospheric temperatures along the horizontal track (including unperturbed profile); Density deviations along the horizontal track (i.e. perturbed over unperturbed density ratios). Profiles obtained at altitude 80000 m, Solar Longitude $L_s=73^\circ$ and a local time of 10 hours.

constituting a horizontal trajectory (varying latitude and longitude) is characterized by the dynamic distance $Dist$, representative for the wave propagation direction, and calculated between the trajectory's initial point (lat_0, lon_0) and its following points (lat, lon) (where lat and lon are respectively the latitude and longitude). $Dist$ is expressed as follows:

$$Dist = 2R_{Mars} \arcsin\left(\sqrt{\sin\left(\frac{lat - lat_0}{2}\right)^2 + \cos(lat_0) \cos(lat) \sin\left(\frac{lon - lon_0}{2}\right)^2}\right) \quad (21)$$

The trajectory's initial point (lat_0, lon_0) remains unchanged for a complete set of points launched by the same seed, and is resaved at every new seed launch.

Perturbations to temperature, density and wind at height z are then found by using the value at $z + \delta z$ on the background profile, with the perturbations to temperature and density calculated on the assumption of adiabatic motion to the valid height.

A value can be chosen for λ , (we take $\lambda = 16$ km as a default, as it provides a reasonable comparison with the observed Viking entry temperature profiles above 50 km), in the range of 2-30 km; longer vertical wavelength should be well resolved by the model and shorter wavelengths result in negligible perturbations. By fixing the value of λ , the user will also fix the one of λ_{Dist} , such as $\lambda_{Dist} = 10 \times \lambda$, which is a realistic order of magnitude based on observations.

The amplitude of the waves, growing with the altitude, is limited by a maximum value of δz , δz_{max} , corresponding to their saturation. δz_{max} is randomly varying between $\frac{\lambda}{2\pi}$ and $3 \times \frac{\lambda}{2\pi}$, which seems reasonable according to available observations (aerobraking data from MGS, MRO, ODY, and datasets of the mass spectrometer NGIMS on board MAVEN).

An example of several small scale perturbations is shown in Figures 9 and 10 .

6 High Resolution Outputs

The Mars Climate Database has been compiled from the output of a general circulation model in which the topography is very smoothed because of its low resolution. In addition, the pressure variations due to the CO₂ cycle (condensation of atmospheric CO₂ in the polar caps) that is computed by the model is only based on the simulation of the actual physical processes. The polar cap physical properties have been tuned somewhat to reproduce the observations, but no correction was added.

The access software includes a “high resolution” mode which combines high resolution (32 pixels/degree) MOLA topography and the smoothed Viking Lander 1 pressure records (used as a reference to correct the atmospheric mass) with the MCD surface pressure in order to compute surface pressure as accurately as possible. The latter is then used to reconstruct vertical pressure levels and hence, within the restrictions of the procedure, yield high resolution interpolated values of atmospheric variables.

All these post-processing procedures are detailed in the following subsections.

6.1 High Resolution Topography and Areoid

The MCD includes (and uses) topography and areoid (Mars geoid) at the database’s resolution (64 × 49 in longitude × latitude). The need to yield higher resolution outputs has led to the development of post-processing tools which require knowledge of these two fields at a much higher resolution. This is achieved using the most up-to-date models and datasets distributed by the Mars Orbiter Laser Altimeter (MOLA) Team.

6.1.1 Mars Gravity Model

Very high resolution values of the Martian areoid can be computed using the MGM1025 spherical harmonic solution of the Mars gravity field to degree and order 80, using X band tracking data of the MGS Mars Orbiter Laser Altimeter. This model is an update of the Goddard Mars Model 2B (GMM2B) described in Lemoine et al. (*J. Geophys. Res.*, 106(E10), 2001) and follows the IAU2000 rotation model and cartographic frame (see Seidelmann et al., *Cel. Mech. Dyn. Astron.*, 82, 83-110 2002) recommended by the Mars Cartography Working Group.

A Fortran program to compute the radius of the geoid at given areocentric latitude and longitude, along with a file containing the MGM1025 coefficients, are kindly made available by G. Neumann from:

<http://ltpwww.gsfc.nasa.gov/tharsis/data.html>

The supplied `areoid.f` program was adapted and merged into the MCD `heights.F` collection of routines which uses the MGM1025 gravity field coefficients (file `mgm1025` in `data` directory of the MCD obtained from the same source).

6.1.2 MOLA Topography

The MOLA Precision Experiment Data Record (PEDR) are archived and distributed by the Planetary Data System (<http://pds.jpl.nasa.gov>) and include topography data binned at various resolutions (from 4 pixels per degree to 128 pixels per degree for the whole planet and up to 512 pixels per degree in the polar regions).

The 32 pixel per degree topography file (a binary file) was converted to NetCDF, yielding the ‘`mola32.nc`’ file (in the `data` directory of the MCD) which is used by MCD software. The choice of this resolution as “high resolution” results from a compromise between datafile size and need for resolution (32 pixels per degree corresponds to a 1850 m resolution at the equator, where the mesh is largest): the file `mola32.nc` is already a 127 Mb file (a higher resolution 64 pixels per degree topography file would be 4 times bigger, i.e. around 520 Mb).

6.2 Deriving High Resolution Surface Pressure

High resolution surface pressure may be obtained from GCM surface pressure by using Viking Lander 1 records to correct atmospheric mass and by taking into account the change in altitude from the (coarse and smoothed) GCM topography to more realistic high resolution topography.

In practice, an estimation of the high resolution surface pressure P_s at a given location and time is given by:

$$P_s = P_{S_{\text{GCM}}} \frac{\langle P_{\text{VL1OBS}} \rangle}{\langle P_{\text{VL1GCM}} \rangle} e^{-(z-z_{\text{GCM}})/H} \quad (22)$$

where $P_{S_{\text{GCM}}}$ is the pressure predicted by the GCM at the same location and time (bilinear interpolations from the MCD grid), $\langle P_{\text{VL1OBS}} \rangle$ the VL1 surface pressure records smoothed to remove thermal tides and transient waves, $\langle P_{\text{VL1GCM}} \rangle$ the similarly smoothed (i.e. diurnally averaged) VL1 surface pressure predicted by the GCM (interpolated vertically and horizontally), z is the altitude of the local surface retrieved from the MOLA dataset, and z_{GCM} is the altitude at the location interpolated from the coarse GCM topography grid. H is the scale height used in the hydrostatic equation to vertically interpolate the pressure: $H = RT/g$ with R ($\text{m}^2 \text{s}^{-2} \text{K}^{-1}$) the gas constant, $g = 3.72 \text{ m s}^{-2}$ the acceleration of gravity, and T the atmospheric temperature extracted from the GCM at about 1 km above the surface⁷. The choice of this altitude to interpolate surface pressure on Mars is based on the theoretical considerations and tests described in Spiga et al. (*J. Geophys. Res.*, 112, E08S16, 2007).

This procedure to predict high resolution surface pressure was initially provided with Mars Climate Database version 4.1, as a distinct external tool, ‘pres0’. As of version 4.2 and 5. of the MCD, the main routine ‘call_mcd’ can yield high resolution outputs and uses the procedure described above to derive high resolution surface pressure values. The ‘pres0’ tool is still provided as a standalone tool (which uses data files `VL1.1s`, the smoothed VL1 surface pressure, `mola32.nc` for the high resolution topography and file `ps_MY24.nc` which simply contains the minimal subset of data from the MCD required for the algorithm).

An example of the impact of the high resolution scheme is given in Figure 11 where are plotted the surface pressure, at GCM resolution, at VL1 site along with the pressure (at the same elevation) that is obtained (see next section) from the high resolution surface pressure derived using the scheme described above. Note that due to the “total atmospheric mass correction” term, the $\langle P_{\text{VL1OBS}} \rangle / \langle P_{\text{VL1GCM}} \rangle$ ratio in Eq. 22, the difference between GCM resolution and high resolution pressures at a fixed location varies non-monotonically with solar longitude.

6.2.1 Deriving high resolution pressure for the dust storm cases

As can be seen in the left panel of Figure 12, the evolution of the pressure cycle was strongly altered at VL1 site, with respect to the annual pressure cycle of the “clim” scenario. The Viking Lander 1 records however show little change in observed trends of annual pressure cycle with the occurrence or not of global dust storms.

Since there are other locations (see right panel of Figure 12) on the planet which display less deviation of the annual pressure cycle when a global dust storm is simulated, we have chosen to use one of these (grid point located at longitude= 0, latitude= -45) as a synthetic Viking Lander 3 record (obtained using the high resolution scheme described above, for the climatology scenario). The later is then used, instead of VL1 data, when deriving high resolution pressure for the dust storm scenarios.

⁷Technically, the temperature that is used is that of the 7th atmospheric layer, which is located at about 1 km above the surface (see Section 2.4.2).

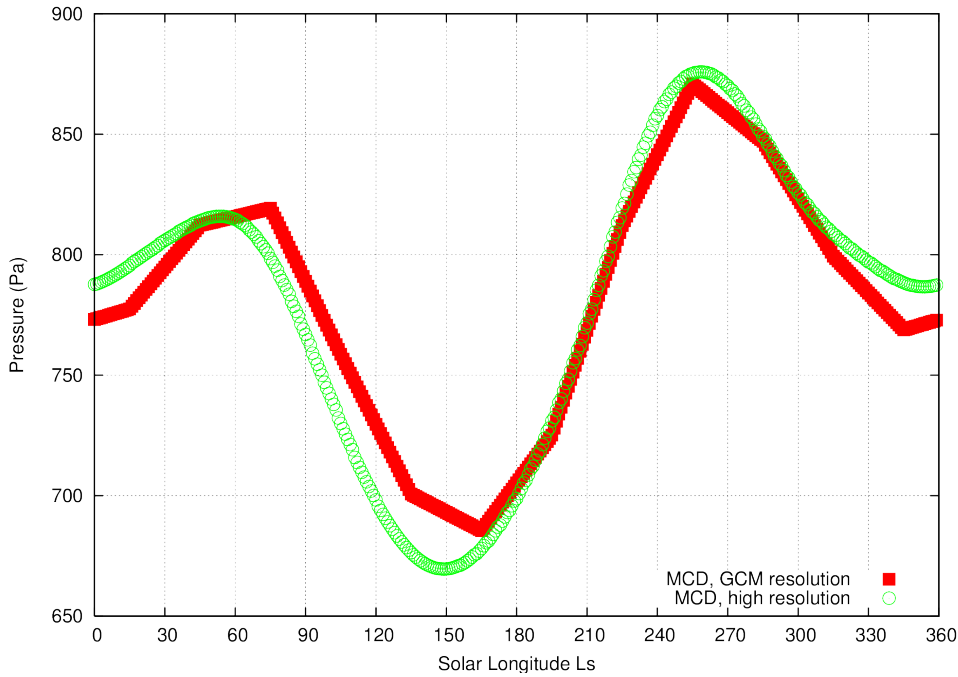


Figure 11: Illustrative example of the effect of the high resolution mode: Pressure at VL1 location (longitude -47.949619° east and latitude 22.269628° north) and at altitude -3421.1113 m above areoid (which corresponds to the surface at GCM resolution; at high resolution the surface lies at -3637.1396 m above areoid).

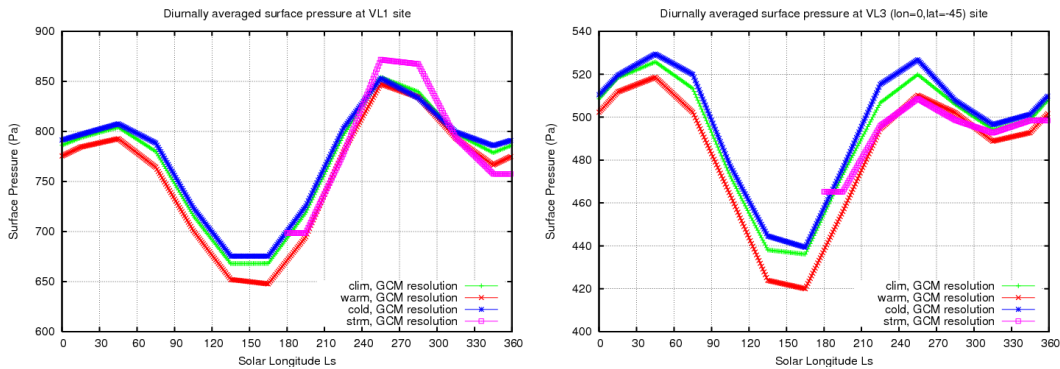


Figure 12: Left: Diurnal surface pressure in the MCD at GCM grid point close to VL1 site, obtained for the clim, cold, warm and storm dust scenarios. Right: Diurnal surface pressure in the MCD at a grid point located at longitude 0 and latitude 45S, for the same simulations, showing that this point would be a better reference (i.e. a fictitious VL3 record) to use (rather than VL1) to compute high resolution surface pressure in the dust storm case.

6.3 Computing High Resolution Values of Atmospheric Variables

6.3.1 Interpolation of Atmospheric Temperature

The MCD contains the atmospheric temperatures obtained from the corresponding GCM runs, on the same grid (as described in Section 2.4), and thus at given pressure $P(l)$ for a given location and layer l (computed from surface pressure $P_{S_{\text{GCM}}}$ interpolated from the 3.75° latitude by 5.625° longitude 64×49 MCD grid, using Equation 1 as shown in Section 2.4.2). If, however, the surface pressure should in fact be $P_{S_{\text{HR}}}$, as given by Equation 22, then a legitimate question is then: How should the atmospheric temperature profile $T(l)$ above $P_{S_{\text{HR}}}$ be interpolated?

To better understand this issue, i.e. the behavior of atmospheric temperature field over topography at higher resolutions, high resolution simulations (176×132 at LMD and up to 512×256 at The Open University) were performed and their output compared to the lower (64×49) resolution ones.

These simulations show that temperature behaves as follows :

1. When topography -and thus surface pressure- varies locally, surface temperature is not affected (it is in radiative equilibrium; only the variation of dust opacity affects the surface temperature, but the impact should be small compared to the variations of albedo, thermal inertia, and slope).
2. To first order, temperature near the surface (first few kilometres) is controlled by the distance from the surface. Above, it is controlled by the pressure level, somewhat independently from the kilometre scale topography.
3. To second order, the near surface air temperature is colder in high altitude regions than in the neighbouring plains, as a result of adiabatic cooling.
4. In local depressions (crater, canyon, etc.), the opposite effect is observed (near surface air warming) but it is less significant.

These facts are taken into account to build the rules to use to interpolate temperature in “high resolution” mode: The MCD temperature profile $T(l)$ is not changed, but the corresponding pressure levels $P(l)$ are. Doing so moreover enables the use of the same database access software as with the “low resolution”, except for the adjustment of pressure levels.

After a bit of tuning and applying rules 1 to 4 above, it has been found that the new “high resolution” pressure levels $P_{HR}(l)$ can be built using a function designed to ensure a smooth transition from the near-surface conditions to the free atmosphere (high altitude) environment:

$$P_{HR}(l) = P_{GCM}(l) [f(l) + (1 - f(l)) 0.5 (1 + \tanh(6 (-10 \ln(\frac{P_{GCM}(l)}{P_{SGCM}}) - z)/z))] \quad (23)$$

where $P_{GCM}(l)$ is the original pressure level in the database. z roughly corresponds to the altitude above the surface (in the GCM smoothed topography) where P_{HR} will become equal to P_{GCM} . It varies depending on the altitude difference (derived from pressure) between the high and low resolution grid Δz (km) :

$$\Delta z = -10 \ln \left(\frac{P_{S_{HR}}}{P_{S_{GCM}}} \right) \quad (24)$$

And z is set to:

$$\begin{aligned} z &= \Delta z + 3 \text{ if } \Delta z > 0 \text{ (local mountain)} \\ z &= 3 \text{ if } \Delta z < 0 \text{ (local depression)} \end{aligned}$$

$f(l)$ is a variable parameter which is equal to 1 at high altitude (then $P_{HR}(l) = P_{GCM}(l)$). At low altitude, it is designed to ensure that the first levels will be at the same distance from the surface in both low and high resolution (then $P_{HR}/P_{S_{HR}} = P_{GCM}/P_{S_{GCM}}$ except when there is a local high topography structure (HR surface more than 1 km above the GCM surface). In such conditions the model levels are compressed closer to the surface, to mimic the observed behaviour in high resolution GCM simulations. Conversely the model levels are expanded when there is a topographic low. (HR surface more than 1 km below the GCM surface). In practice $f(l)$ is computed as:

$$f(l) = \frac{P_{S_{HR}}}{P_{S_{GCM}}} \left(\frac{P_{GCM}(l)}{P_{S_{GCM}}} \right)^x \quad (25)$$

where x is the parameter which controls the compression or the extension of the layers near the surface (no effect when $x = 0$, compression if $x < 0$, extension if $x > 0$).

The value of x is derived from that of Δz :

$$\begin{aligned}
x &= 0 && \text{if } -1 < \Delta z < 1 \\
x &= -0.12 (|\Delta z| - 1) && \text{if } \Delta z > 1 \\
x &= +0.12 (|\Delta z| - 1) && \text{if } \Delta z < -1 \\
x &= 0.8 && \text{if formulas above yield } x > 0.8 \\
x &= -0.8 && \text{if formulas above yield } x < -0.8
\end{aligned}$$

Figures 13 and 14 display examples of the temperature fields produced by the “high resolution” MCD V4.2 compared to the “low resolution” version and true high resolution (176×132) GCM output.

6.3.2 Interpolation of Density

In the low resolution version of the database, the density ρ (kg m^{-3}) at altitude z (m) is interpolated in the vertical by using a weighted interpolation between the density at the level above (ρ_{l+1}) and the density at the level below (ρ_l). In practice the linear interpolation is performed on the logarithm of the density (as mentioned in Section 4.2.2).

Density is proportional to pressure and thus, in the “high resolution” mode, it must be recomputed by taking into account the change in pressure (computed using Equation 23). The algorithm for vertical interpolation that is used for “low resolution” density is used to compute “high resolution” density, but using $\rho_{l+1}P_{\text{HR}}(l+1)/P_{\text{GCM}}(l+1)$ and $\rho_l P_{\text{HR}}(l)/P_{\text{GCM}}(l)$ instead of ρ_{l+1} and ρ_l

A similar treatment is applied to the RMS of density, corresponding perturbations, etc...

6.3.3 Modification of Other Variables

Most other atmospheric variables X (winds, turbulent kinetic energy, gases and ice mixing ratio) are treated like temperature: the values of the profile $X(l)$ are kept, and only the pressure of the levels $P(l)$ are recomputed to account for the “high resolution” post-processing.

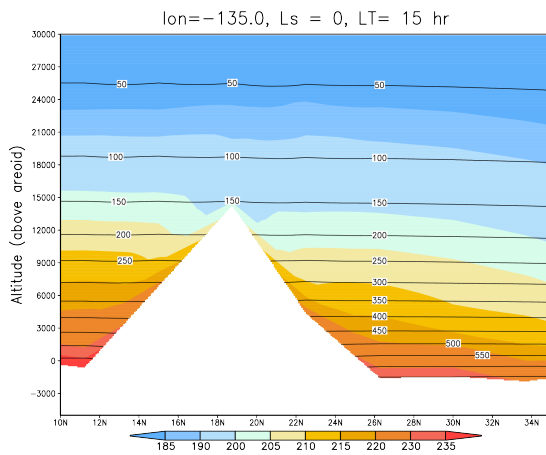
The dust optical depth τ is scaled to the high resolution surface pressure (e.g. $\tau_{\text{HR}} = \tau_{\text{GCM}} P_{\text{S}_{\text{HR}}}/P_{\text{S}_{\text{GCM}}}$).

Column densities properly integrated in low resolution are already stored in the MCD data files. In order to get columns for the high resolution surface pressure, the two columns are roughly integrated over high and low resolution sigma levels based on the hydrostatic equation:

$$\begin{aligned}
c_{\text{GCM}}^j &= \sum_{l=2}^{l=L} \{ (\text{vmr}^j(l) R_{\text{m}}(l) [P_{\text{GCM}}(l-1) - P_{\text{GCM}}(l)]) / (g_{\text{m}}(l) k_{\text{b}}) \} \\
c_{\text{HR}}^j &= \sum_{l=2}^{l=L} \{ (\text{vmr}^j(l) R_{\text{m}}(l) [P_{\text{HR}}(l-1) - P_{\text{HR}}(l)]) / (g_{\text{m}}(l) k_{\text{b}}) \}
\end{aligned} \tag{26}$$

where vmr^j is the volume mixing ratio of specie j , k_{b} is the Boltzmann constant. Then to scale to the high resolution surface pressure the low resolution column density from the MCD data files is multiplied by the ratio $c_{\text{HR}}/c_{\text{GCM}}$.

DAY



NIGHT

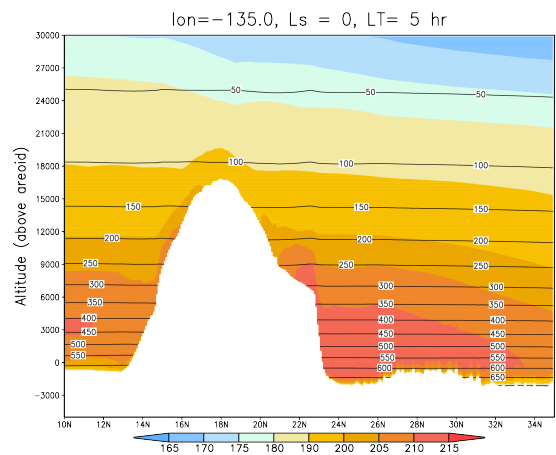
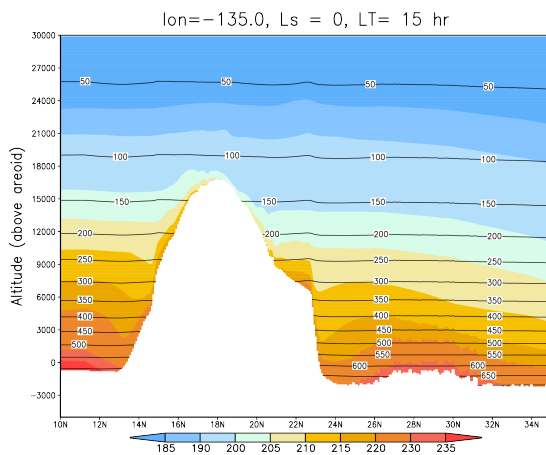
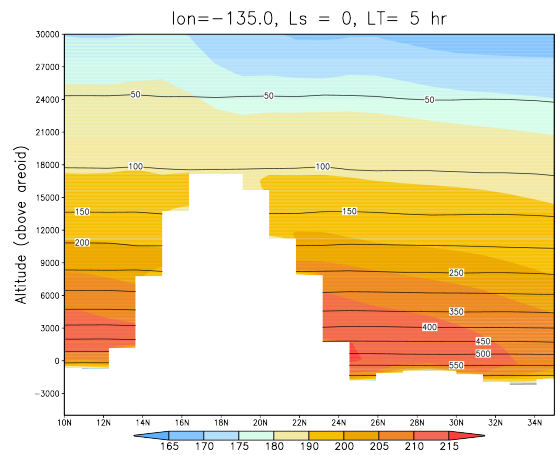
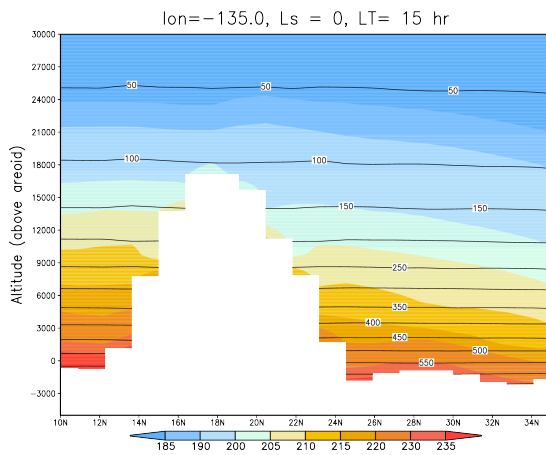
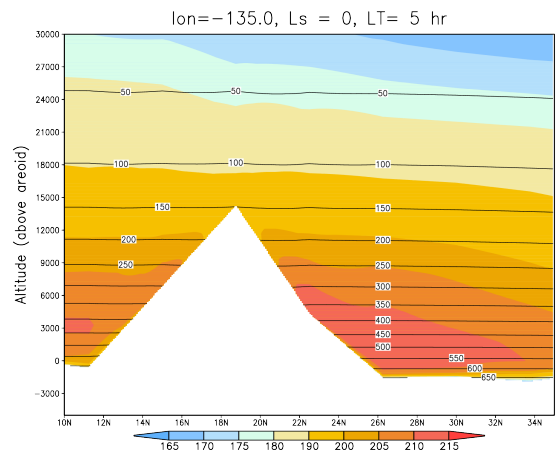
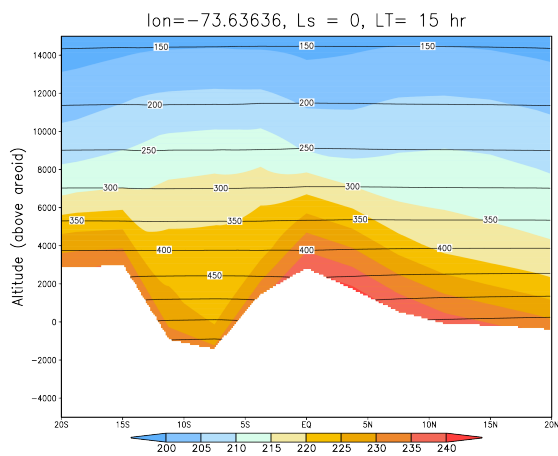


Figure 13: Cross-section of temperature fields (colored) and pressure level (black contour) near Olympus Mons from the MCD at GCM resolution (top row), from a high resolution 176×132 GCM run (middle row), and from the high resolution output of the MCD (bottom row). Note that there is an order of magnitude between horizontal and vertical scales in these plots; what appear as sharp gradients in the horizontal direction are in fact quite smooth when displayed using more commensurate axes.

DAY



NIGHT

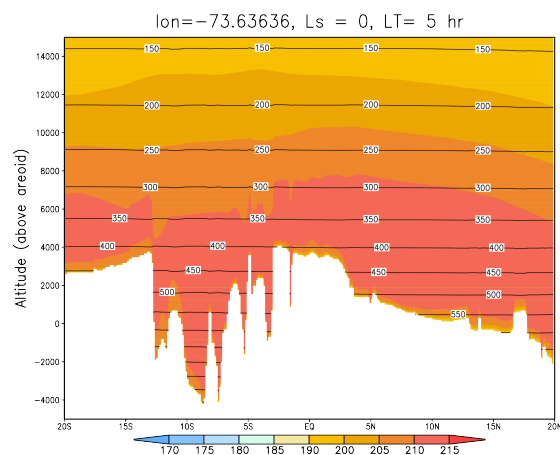
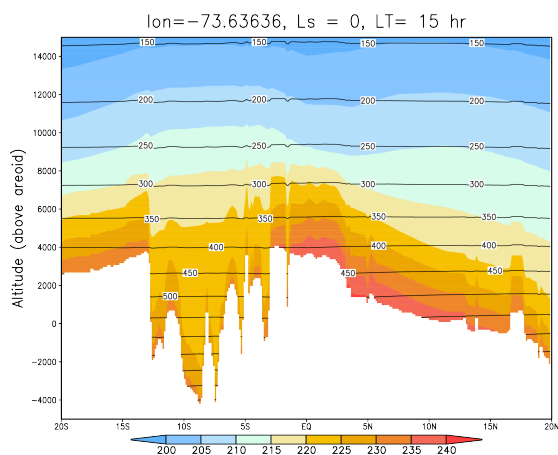
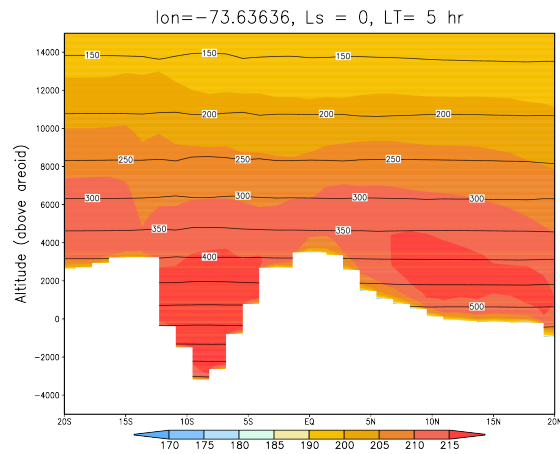
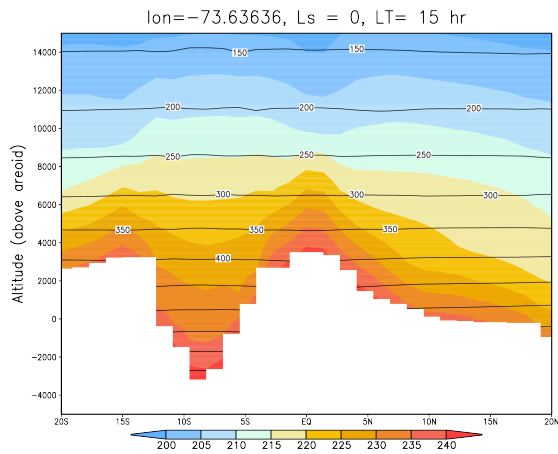
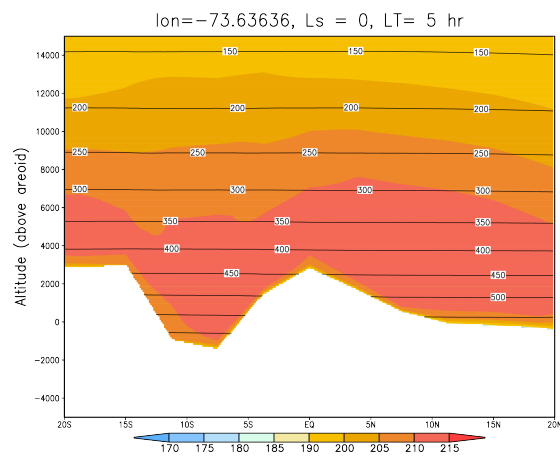


Figure 14: Cross-section of temperature fields (colored) and pressure level (black contour) near Valles Marineris from the MCD at GCM resolution (top row), from a high resolution 176×132 GCM (middle row), and from the high resolution output of the MCD Note that there is an order of magnitude between horizontal and vertical scales in these plots; what appear as sharp gradients in the horizontal direction are in fact quite smooth when displayed using more commensurate axes.

A Computing Martian Dates and Local Time

In this appendix we briefly describe how one may compute aerocentric solar longitude of Mars for a given Julian date, as well as how to compute corresponding Local True Solar Time.

The equations and methods given here are taken from Capderou (2005) which should be consulted for a detailed description.

A.1 Some constants

N_s	88775.245	Number of seconds in a sol (martian day)
	668.6	Number of sols in a martian year
Ls_{peri}	250.99	Perihelion date (in deg.)
t_{peri}	485.35	Perihelion date (in sols)
a	1.52368	Semi-major axis of orbit (in AU)
e	0.09340	Orbital eccentricity
ϵ	25.1919	Obliquity of equator to orbit (in deg.)

A.2 Computing martian dates and aerocentric solar longitude

A.2.1 The three anomalies

For an elliptical trajectory, the **true anomaly** ν is given by the polar angle of the position, with the convention that $\nu = 0$ at the periastron (minimum distance to center, i.e. the perihelion, in Mars' case).

If $n = 2\pi/T$ is the mean angular frequency of motion (T is the period of revolution, i.e. a year), then at time t (taking the time origin as $t = t_{peri}$, perihelion date at which $\nu = 0$):

$$n(t - t_{peri}) = 2 \arctan \left[\sqrt{\frac{1-e}{1+e}} \tan \frac{\nu(t)}{2} \right] - \frac{e\sqrt{1-e^2} \sin \nu(t)}{1+e \cos \nu(t)} \quad (27)$$

The **eccentric anomaly** E is related to mean motion n by:

$$n(t - t_{peri}) = E(t) - e \sin E(t) \quad (28)$$

The **mean anomaly** M is the angle determining the position of a fictitious point in uniform circular motion of angular frequency n . Thus,

$$n(t - t_{peri}) = M(t) \quad (29)$$

A.2.2 Aerocentric solar longitude Ls

The position of the planet on its heliocentric orbit is given by the aerocentric solar longitude Ls . The origin of Ls is defined as the vernal equinox (northern hemisphere spring equinox).

Ls is directly related to the true anomaly ν :

$$\nu = Ls - Ls_{peri} \quad (30)$$

where Ls_{peri} is the perihelion date.

A.2.3 Converting Julian date JD to Martian sol number D_s

For a given Julian date JD , the corresponding martian sol date $D_s \in [0; N_s]$ (i.e. number of sols elapsed since beginning of martian year defined by $L_s = 0$):

$$D_s = (JD - JD_{ref}) \frac{86400}{88775.245} \pmod{N_s} \quad (31)$$

where 86400 and 88775.245 are respectively the number of seconds in an earth day and a martian sol. JD_{ref} is a reference Julian date corresponding to an $L_s = 0$ event.

Example of reference date: $L_s = 0$ occurred on 19-12-1975 at 4:00:00, which corresponds to Julian date 2442765.667.

A.2.4 Converting sol number D_s date to L_s

For a given sol number $D_s \in [0; N_s]$, the corresponding value of aerocentric solar longitude L_s may be computed as follows:

Step 1: Compute mean anomaly $M(D_s)$ (in radians):

$$M = 2\pi \frac{D_s - t_{peri}}{N_s} \quad (32)$$

Step 2: Compute eccentric anomaly $E(D_s)$ (in radians):

This is the tricky bit (also known as Kepler's problem). Eccentric and mean anomalies are related by the nonlinear equation:

$$M = E - e \sin E \quad (33)$$

which must be solved by, for instance, a Newton iterative procedure.

Step 3: Compute true anomaly $\nu(D_s)$ (in radians) using:

$$\nu = 2 \arctan \left[\sqrt{\frac{1+e}{1-e}} \tan \left(\frac{E}{2} \right) \right] \quad (34)$$

Step 4: Compute $L_s(D_s)$ (in degrees):

$$L_s = \left(\nu \frac{180}{\pi} + L_{speri} \right) \pmod{360} \quad (35)$$

A.3 Computing Local True Solar Time

The steps required to compute the Local True Solar Time at a given longitude lon (in degrees East) for a given Julian Date are the following:

Step 1: Compute Local Mean Time LMT_0 at longitude 0, in martian hours, for a given Julian date JD :

$$LMT_0 = \left(LMT_{ref} + 24(JD - JD_{ref}) \frac{86400}{88775.245} \right) \pmod{24} \quad (36)$$

Where JD_{ref} is a reference Julian date, and LMT_{ref} the Local Mean Time at longitude 0, in martian hours, at that date. 86400 and 88775.245 are respectively the number of seconds in an earth day and a martian sol.

Example of reference date and time: 01-01-1976 at 00:00:00 was such that $JD_{ref} = 2442778.5$ and $LMT_{ref} = 16.1725$.

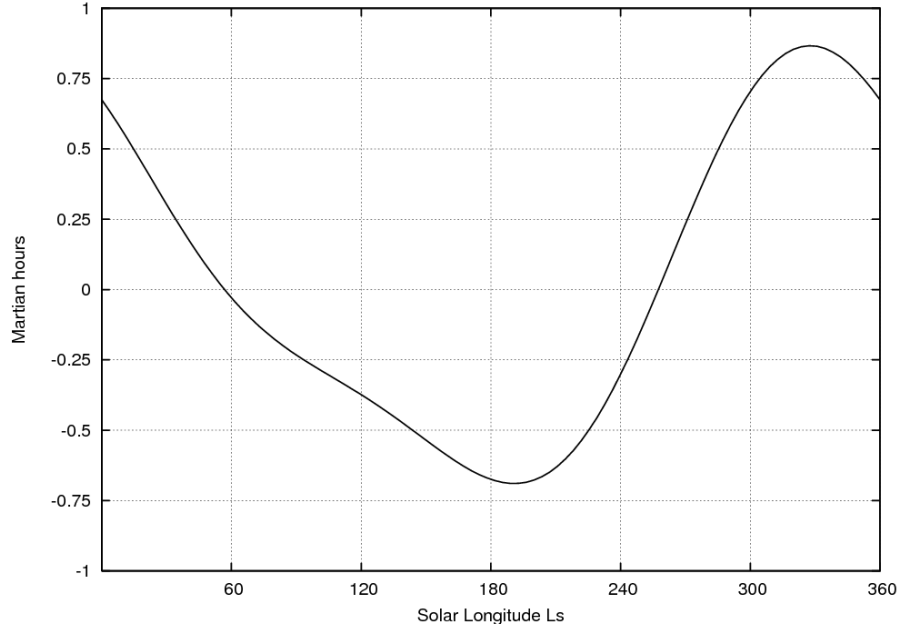


Figure 15: Equation Of Time (EOT) for Mars, showing the difference between Mean Local Time and True Solar Time, as a function of Solar Longitude L_s .

The equation above assumes simple Keplerian motion and is accurate to a few minutes with respect to more advanced computations which account for the interactions between main objects of the Solar System (see e.g. the "Mars24" website <http://www.giss.nasa.gov/tools/mars24> and documentation).

As of MCDv5.2 and the following version, we use a more elaborate equation to compute LMT_0 for a given JD , as can be seen in the `Mars_LMT0` function in `call_mcd.F` where small corrections are added to obtain a better match with the full computation from "Mars24". We thus obtain a result shown to be accurate to a second or less over the period of Earth years 1950 to 2050.

Step 2: For the given aerocentric solar longitude L_s (which is obtained from Julian Date JD as explained previously), compute the Equation Of Time EOT (which yields, in martian hours, the difference between Mean Time and True Solar Time; see Figure 15) :

$$EOT = \left[2e \sin(L_s - L_{s_{peri}}) - \tan^2\left(\frac{\epsilon}{2}\right) \sin(2L_s) \right] \frac{24}{2\pi} \quad (37)$$

Where $L_{s_{peri}}$ is the perihelion date, e the orbital eccentricity and ϵ the obliquity of equator to orbit.

Step 3: Compute Local True Solar Time at longitude 0, $LTST_0$, in martian hours:

$$LTST_0 = LMT_0 - EOT \quad (38)$$

step 4: At longitude lon (in degrees east), Local True Solar Time $LTST$, in martian hours, is then:

$$LTST = \left(LTST_0 + \frac{lon}{15} \right) (mod\ 24) \quad (39)$$

B Differences Between Version 5.3 and Previous Versions of the MCD

Differences between version 5.3 and version 5.2

- New EUV min/max/ave scenarios: the bracketing and average Extreme UV forcings from the Sun have been redesigned to be more in line with our knowledge of the recent solar cycles.
- The added small scale perturbation (gravity waves) scheme has been improved to also take into account the horizontal propagation of the gravity wave.
- The evaluation of species column amount, when in high resolution mode, has been improved.
- The extrapolation of density and species volume mixing ratio when above the MCD topmost layer (250km) has been improved.
- The scenario for Mars Year 32 has been added.
- The Matlab interface has been improved and is now fully interactive.
- The values of water ice effective radius (`extvar[45]`) were wrong in MCDv5.2 and have been corrected.

Differences between version 5.2 and version 5.1

- The main changes in MCD version 5.2 are the addition of add-on scenarios for Mars Years 24 to 31, and important fixes concerning vertical velocity, total electronic content and interpolations in the near-surface layer.
- Overall, all the changes that have been introduced are:
 - Added scenarios for Mars Years 24 to 31 (corresponding to values 24 to 31 for `call_mcd` input `scena` parameter).
 - Vertical velocity and associated RMS (`extvar[26]` and `extvar[27]`) have been corrected.
 - Total electronic content (TEC, `extvar[76]`) is better evaluated (using "chemistry ionosphere" electronic content only).
 - The interpolation scheme for the near-surface layer (first few meters above the surface) has been improved.
 - More control when using combined small and large scale perturbation schemes to avoid (rare cases of) unphysically negative density.
 - Added Local Mean Solar Time to outputs (`extvar[11]`)
 - Added Sun-Mars distance to outputs (`extvar[12]`)
 - Added solar zenith angle to outputs (`extvar[56]`)

Differences between version 5.1 and version 5.0

- The main change in MCD version 5.1 is in generation of the underlying dust scenarios to better represent the baseline Martian climatology (scenario "clim", now based on a geometrical mean of several years opacities) and extreme bracketing cases: "cold" (now without radiatively active clouds), "warm", "storm"
- Other changes that have been introduced are:
 - In the MCD software: A near-surface variability scheme has been added to better account for the sub-grid scale effects in the MCD perturbation schemes.

- In the MCD software: Improved interpolation between the surface and the model lowest layer (5 m) for temperature and winds.
- In the MCD software: several changes in the output variables array *extvar*, as detailed in the *MCD v5.1 User Manual*.
- In the GCM: The mean atmospheric composition in Ar and N₂ has been updated to match the latest (2013) Curiosity SAM measurements.
- In the GCM : Better representation of the water cycle yielding some improvements in the prediction of water vapor, ice and ice particle radii.
- In the GCM: Improved representation of the extreme UV flux from the Sun.
- In the GCM: Corrected Boundary layer (nighttime surface layer)
- In the GCM: Corrected Dynamical scheme (on potential temperature) when CO₂ is condensing or subliming.

Differences between version 5.0 and version 4.3

- The main change in MCD version 5.0 is in the fact that the database files result from simulations using the a completely **new version of the LMD GCM**, which includes many improvements, compared to the version that was used to derive MCDv4.x datafiles. In particular: radiatively active clouds, improved clouds microphysic, semi-interactive dust transport, new dust radiative properties, improved CO₂ cycle, improved convective boundary layer, ionosphere, improved NLTE cooling in the upper atmosphere, etc.
- Other changes which have been introduced are:
 - The EOFs (Empirical Orthogonal Functions) for large scale perturbation scheme are now at higher resolution (32×24; twice what was used previously). Moreover, for the “climatology” scenario, EOFs corresponding to the individual (Mars Years 24, 26, 27, 29 and 30) runs are used.
 - Improved interpolation between the surface and the model lowest layer (5 m) for temperature and winds.
 - Many new variables have been included: Columns and volume mixing ratios of Ar, O, O₂, H, H₂, electrons, key parameters concerning the convective planetary boundary layer (PBL), etc.
 - Users may now pick which “extra variables” need be computed and outputed (rather than the all-or-nothing capability of previous MCD software).

Differences between version 4.3 and version 4.2

- The main upgrade in MCD version 4.3 is the improvement of the large scale perturbation model. Version 4.3 thus uses the same database datafiles as version 4.2, except for a subset which contains updated data required for the large scale perturbation model.
- Other changes that have been introduced are:
 - An additional vertical coordinate (‘zkey’ parameter) may be used to specify vertical coordinate as altitude above reference radius (arbitrarily set to 3.39610⁶ m).
 - The output unit to which messages are written is now a parameter that can be set by the user (the default output unit is set to 6, which implies, in conformance with Fortran standards, the standard output).
 - In order for the whole MCD to fit in a single DVD, some datafiles (all those which contain data about dust storm scenarios, i.e. files in the `data` directory with names starting with `strm`) have been compressed (gzipped) and should be un-compressed (gunzipped) before being used.

Differences between version 4.2 and version 4.1

- Version 4.2 uses the same database datafiles as version 4.1, except for a small subset (the files which contain variability); most improvements, changes and new features are in the access and postprocessing software.
- The main new features and differences are:
 1. The main Fortran subroutine to retrieve data from the database is now called “call_mcd” and **significant changes to the argument list**, compared to its predecessor “atmemcd”, have been introduced:
 - A new high resolution procedure (based on the integration of high resolution 32 pixels per degree MOLA topography) has been implemented.
 - Input and output arguments which are floating numbers are now declared as **single precision** (i.e. Fortran REAL), except ‘xdate’, which is double precision, (i.e. Fortran REAL*8).
 - The way by which users impose date and local time has changed.
 - Input **longitude and latitude must now be given in degrees**. Longitude is interpreted as degrees east (as before).
 - Input arguments used to signal and generate perturbations have been changed.
 - Day to day variability of atmospheric variables is now given either pressure-wise or altitude-wise, depending on the vertical coordinate selected by the user.
 2. Examples of interface software for C, C++ and Scilab users, have been added (in addition to the pre-existing IDL and Matlab ones).
 3. Computation of solar longitude (from a given Julian date) has been made more accurate. Computation of local time (given in true solar time) has been improved by using an appropriate equation of time.
 4. The “pres0” tool has been updated.

Lists of changes and improvements of previous versions of the MCD

- Version 4.1 is similar to beta version 4.0 with some improvements and a few problems fixed.
- The main differences between version 4 and previous version 3.1 are:
 1. The database now extends up to the thermosphere and new variables (upper atmospheric composition: CO₂, N₂, CO, O, H₂ and, in the lower atmosphere: water, water ice, ozone, dust) are available.
 2. Different vertical coordinates may be specified as input, including pressure level.
 3. A linear interpolation in time (Ls) for mean variables between seasons was added.
 4. For some variables, an estimation of the “day to day” variation is provided (root mean square values).
 5. There is a significant re-arrangement of arguments of atmemcd so that all the input variables are followed by all the output variables.
 6. We suggest the use of direct compilation rather than using the UNIX command “make”.
 7. Variables are now saved in atmemcd to fix problems with F77 compilers which don’t store values of variables between subroutine calls.
 8. The database now has a more accurate representation of gravity; the fact that it varies following an inverse square law is accounted for when integrating the hydrostatic equation. The variation of R, the gas constant, with altitude is also taken into account.

9. The horizontal resolution of the database has changed to $5.625^\circ \times 3.75^\circ$ (longitude \times latitude).
 10. We now provide the separate tool to compute surface pressure with high accuracy.
 11. We now provide some tool to use the database software from IDL.
- A major change in Version 3.1, compared to version 3.0 of the database, is the change from DRS data format to NetCDF. A bug was also fixed for the calculation of large scale variability in the upper atmosphere (above 120 km).
 - The main differences between version 3.0 and 2.3 are mostly related to the content of the database files, due in particular to improvements made in the models used to build the database, including an extension of the model top from 80 to 120 km, improved surface properties and a dust scenarios from Mars Global Surveyor.
 - The main difference between version 2.3 and 2.0 is the use of the main subroutine ATMCD which computes meteorological variables from the Mars Climate Database (MCD).
 - The main difference between version 2.0 and 1.0 of the MCD is that the large-scale variability model now makes use of two-dimensional, multivariate Empirical Orthogonal Functions (EOFs). These now describe correlations in the model variability as a function of both height and longitude (rather than solely of height as in version 1.0).